

Report No. UT-25.19

# **MODELING THE DYNAMIC MODULUS OF ASPHALT MIXTURES USING SINGLE- VALUE TEST RESULTS**

## **PHASE III: DEVELOPMENT OF LOW- TEMPERATURE, HIGH-FREQUENCY RELATIONS**

### **Prepared For:**

Utah Department of Transportation  
Research & Innovation Division

**Final Report  
August 2025**

## **Disclaimer**

The authors alone are responsible for the preparation and accuracy of the information, data, analysis, discussions, recommendations, and conclusions presented herein. The contents do not necessarily reflect the views, opinions, endorsements, or policies of the Utah Department of Transportation or the U.S. Department of Transportation. The Utah Department of Transportation makes no representation or warranty of any kind, and assumes no liability therefore.

## **Acknowledgments**

The authors acknowledge the Utah Department of Transportation (UDOT) for funding this research and the following individuals from UDOT on the Technical Advisory Committee for helping to guide the research:

- David Stevens
- Jason Simmons
- Craig Hebbert
- Howard Anderson

The following students from the University of Utah are an integral part of this work:

- Fatoumata Binta Barry
- Ian Cleave

Materials were graciously provided by the Minnesota Department of Transportation from their research sections at MnROAD. Special thanks to Dr. Michael Vrtis for facilitating the materials.

# Technical Report Documentation Page

1. Report No. UT-25.19		2. Government Accession No. N/A		3. Recipient's Catalog No. N/A	
4. Title and Subtitle Modeling the Dynamic Modulus of Asphalt Mixtures Using Single-Value Test Results, Phase III: Development of Low-Temperature, High-Frequency Relations				5. Report Date August 2025	
				6. Performing Organization Code N/A	
7. Author(s) Beatriz Fieldkircher, Jeremiah Adejube, Kevin VanFrank, P.E., and Pedro Romero-Zambrana, Ph.D., P.E.				8. Performing Organization Report No. N/A	
9. Performing Organization Name and Address The University of Utah Department of Civil and Environmental Engineering 110 South Central Campus Drive, Suite 2000 Salt Lake City, UT 84112				10. Work Unit No. 5H094 09H	
				11. Contract or Grant No. 24-8836	
12. Sponsoring Agency Name and Address Utah Department of Transportation 4501 South 2700 West P.O. Box 148410 Salt Lake City, UT 84114-8410				13. Type of Report & Period Covered Final Report Jan 2024 – Aug 2025	
				14. Sponsoring Agency Code PIC No. UT23.102	
15. Supplementary Notes Prepared in cooperation with the Utah Department of Transportation and the U.S. Department of Transportation, Federal Highway Administration					
16. Abstract This research developed a practical method to relate UDOT's existing material tests for asphalt mixtures, including the Bending Beam Rheometer (BBR) for low-temperature behavior and the IDEAL-CT for intermediate-temperature cracking, to the dynamic modulus ( $E^*$ ) master curve required for Level 1 inputs in AASHTOWare Pavement ME®. The proposed approach allows for accurate prediction of $E^*$ using simplified testing, eliminating the need for extensive dynamic modulus testing while preserving reliability for pavement design. Thanks to the advances from this work, it is now possible to use materials with the same properties during all aspects of pavement design and construction, thus allowing for life-cycle cost analysis. Validation of this work using the AASHTOWare Pavement ME® software showed no significant difference in the pavement design when using the simplified method proposed by this work; thus, confirming its suitability for practical implementation. Key benefits of this work include: (1) direct linkage between material properties and pavement design for improved life-cycle cost analysis, (2) use of project-specific data instead of national averages, and (3) a significant reduction in testing time requirements from weeks to days and the corresponding decrease in laboratory effort. Overall, this study offers a streamlined, accurate, and efficient process for estimating dynamic modulus master curves for use in pavement design.					
17. Key Words Asphalt Mixtures, dynamic modulus, testing, pavement design, quality control		18. Distribution Statement Not restricted. Available through: UDOT Research & Innovation Div. 4501 South 2700 West P.O. Box 148410 Salt Lake City, UT 84114-8410 <a href="http://www.udot.utah.gov/go/research">www.udot.utah.gov/go/research</a>		23. Registrant's Seal  N/A	
19. Security Classification (of this report)  Unclassified	20. Security Classification (of this page)  Unclassified	21. No. of Pages  68	22. Price  N/A		

# Table of Contents

Disclaimer .....	i
Acknowledgments .....	i
Technical Report Documentation Page.....	ii
Table of Contents .....	iii
List of Tables .....	v
List of Figures.....	vi
Unit Conversion Factors.....	vii
List of Abbreviations and Acronyms .....	viii
Executive Summary .....	1
Chapter 1.0 Introduction.....	2
1.1 Background .....	2
1.2 Objectives.....	3
1.3 Scope .....	4
1.3.1 Mixture Gradations .....	6
1.4 Outline of Report .....	7
Chapter 2.0 Research Methodology.....	8
2.1 Overview.....	8
2.2 IDEAL-CT and Cracking Tolerance Index.....	8
2.2.1 Test Procedure.....	8
2.2.2 Quality Control .....	10
2.3 Bending Beam Rheometer (BBR).....	10
2.3.1 Test Procedures .....	11
2.3.2 Quality Control .....	12
2.4 Illinois Flexibility Index (SCB-IFIT).....	12
2.5 Asphalt Mixture Performance Test (AMPT) .....	13
2.5.1 Dynamic Modulus Master Curve .....	13
2.6 Relation Between Single Point/Index Tests and Dynamic Modulus.....	14
Chapter 3.0 Data Testing and Analysis .....	16
3.1 IDEAL-CT Testing and Data Analysis.....	16

3.2 Bending Beam Rheometer .....	18
3.2.1 BBR Data Visualization .....	18
3.2.2 BBR Data Analysis .....	20
3.3 Semi-Circular Bending Illinois Flexibility Index Test (SCB-IFIT) .....	23
3.3.1 Testing and Data Analysis .....	24
3.4 Comparison of Tests that Evaluate Cracking .....	26
3.4.1 Comparison to Published Data .....	27
3.5 AMPT .....	29
Chapter 4.0 Model Development .....	32
4.1 Overview .....	32
4.2 Verification of Predictive Relation .....	33
4.3 Incorporation of Low-Temperature Data .....	35
4.3.1 Hirsch Model .....	36
4.3.2 Comparison of Results .....	37
4.4 AASHTOWare Verification .....	39
4.4.1 Fatigue Cracking .....	41
4.4.2 Rutting .....	42
4.5 Review .....	43
Chapter 5.0 Summary and Conclusions .....	45
5.1 Summary .....	45
5.2 Mixture Testing .....	45
5.3 Model Development and Validation .....	46
5.4 Conclusions .....	46
5.5 Limitations and Challenges .....	47
Chapter 6.0 Recommendations and Implementation .....	48
6.1 Recommendations .....	48
6.2 Implementation Plan .....	48
References .....	51
Appendix A: Dynamic Modulus Master Curves .....	53
Appendix B: Data Access .....	59

## List of Tables

Table 1 - Description of Mixtures.....	6
Table 2 - Pearson Correlation Between Variables. ....	17
Table 3 - Descriptive Statistics: Average, Standard Deviation, and Coefficient of Variation (COV) for Stiffness and m-value. ....	19
Table 4 - FI and Fracture Energy for Eight Mixes.....	24
Table 5 - Comparison of Predictions from Tests Developed to Evaluate Cracking .....	27
Table 6 - Comparison of Intermediate-Temperature Test Results .....	28
Table 7 - Comparison of Low-Temperature Test Results.....	29
Table 8 - Dynamic Modulus Data for Mixture #10 (Cell 18).....	30
Table 9 - Dynamic Modulus Data for Mixture #11 (Cell 21).....	30
Table 10 - Master Curve Equation Parameters for the 11 Mixtures. ....	31
Table 11 - Prediction of Beta and Gamma Parameters for Mixes #10 and #11 .....	33
Table 12 - Maximum Dynamic Modulus for Predicted and Measured Values .....	38

## List of Figures

Figure 1 - Gradation Chart of All Mixtures. ....	6
Figure 2 - Graphical Representation of Mixes' CT Index and Fracture Energy. ....	16
Figure 3 - Compact Letter Display Boxplot for Grouping Mixes with Similar IDEAL-CT Index Results. ....	17
Figure 4 - Average Stiffness at 60 s. ....	18
Figure 5 - Average m-value at 60 s. ....	19
Figure 6 - Compact Letter Display Boxplot for Creep Stiffness at 0 °C ....	21
Figure 7 - Compact Letter Display Boxplot for Creep Stiffness at -6 °C ....	21
Figure 8 - Compact Letter Display Boxplot for Creep Stiffness at -12 °C ....	22
Figure 9 - Compact Letter Display Boxplot for Creep Stiffness at -18 °C ....	22
Figure 10 - Compact Letter Display Boxplot for Creep Stiffness at -24 °C ....	23
Figure 11 - Compact Letter Display Boxplot for Flexibility Index and Visualization of Games-Howell Output.....	25
Figure 12 - Compact Letter Display Boxplot for Fracture Energy and Visualization of Tukey-Test Output. ....	26
Figure 13 - Relation Between Fracture Energy and Beta Parameter ....	34
Figure 14 - Relation Between CT Index and Gamma Parameter ....	35
Figure 15 - Comparison of Different Model Predictions for Mix #1 ....	39
Figure 16 - AC Bottom-Up Cracking of Each Mixture Across the Models.....	41
Figure 17 - Rutting of Each Mixture Across the Models ....	42

# Unit Conversion Factors

Units used in this report and not conforming to the UDOT standard unit of measurement (U.S. Customary system) are given below with their U.S. Customary equivalents:

<b>SI* (MODERN METRIC) CONVERSION FACTORS</b>				
<b>APPROXIMATE CONVERSIONS TO SI UNITS</b>				
<b>Symbol</b>	<b>When You Know</b>	<b>Multiply By</b>	<b>To Find</b>	<b>Symbol</b>
<b>LENGTH</b>				
in	inches	25.4	millimeters	mm
ft	feet	0.305	meters	m
yd	yards	0.914	meters	m
mi	miles	1.61	kilometers	km
<b>AREA</b>				
in <sup>2</sup>	square inches	645.2	square millimeters	mm <sup>2</sup>
ft <sup>2</sup>	square feet	0.093	square meters	m <sup>2</sup>
yd <sup>2</sup>	square yard	0.836	square meters	m <sup>2</sup>
ac	acres	0.405	hectares	ha
mi <sup>2</sup>	square miles	2.59	square kilometers	km <sup>2</sup>
<b>VOLUME</b>				
fl oz	fluid ounces	29.57	milliliters	mL
gal	gallons	3.785	liters	L
ft <sup>3</sup>	cubic feet	0.028	cubic meters	m <sup>3</sup>
yd <sup>3</sup>	cubic yards	0.765	cubic meters	m <sup>3</sup>
NOTE: volumes greater than 1000 L shall be shown in m <sup>3</sup>				
<b>MASS</b>				
oz	ounces	28.35	grams	g
lb	pounds	0.454	kilograms	kg
T	short tons (2000 lb)	0.907	megagrams (or "metric ton")	Mg (or "t")
<b>TEMPERATURE (exact degrees)</b>				
°F	Fahrenheit	5 (F-32)/9 or (F-32)/1.8	Celsius	°C
<b>ILLUMINATION</b>				
fc	foot-candles	10.76	lux	lx
fl	foot-Lamberts	3.426	candela/m <sup>2</sup>	cd/m <sup>2</sup>
<b>FORCE and PRESSURE or STRESS</b>				
lbf	poundforce	4.45	newtons	N
lbf/in <sup>2</sup>	poundforce per square inch	6.89	kilopascals	kPa
<b>APPROXIMATE CONVERSIONS FROM SI UNITS</b>				
<b>Symbol</b>	<b>When You Know</b>	<b>Multiply By</b>	<b>To Find</b>	<b>Symbol</b>
<b>LENGTH</b>				
mm	millimeters	0.039	inches	in
m	meters	3.28	feet	ft
m	meters	1.09	yards	yd
km	kilometers	0.621	miles	mi
<b>AREA</b>				
mm <sup>2</sup>	square millimeters	0.0016	square inches	in <sup>2</sup>
m <sup>2</sup>	square meters	10.764	square feet	ft <sup>2</sup>
m <sup>2</sup>	square meters	1.195	square yards	yd <sup>2</sup>
ha	hectares	2.47	acres	ac
km <sup>2</sup>	square kilometers	0.386	square miles	mi <sup>2</sup>
<b>VOLUME</b>				
mL	milliliters	0.034	fluid ounces	fl oz
L	liters	0.264	gallons	gal
m <sup>3</sup>	cubic meters	35.314	cubic feet	ft <sup>3</sup>
m <sup>3</sup>	cubic meters	1.307	cubic yards	yd <sup>3</sup>
<b>MASS</b>				
g	grams	0.035	ounces	oz
kg	kilograms	2.202	pounds	lb
Mg (or "t")	megagrams (or "metric ton")	1.103	short tons (2000 lb)	T
<b>TEMPERATURE (exact degrees)</b>				
°C	Celsius	1.8C+32	Fahrenheit	°F
<b>ILLUMINATION</b>				
lx	lux	0.0929	foot-candles	fc
cd/m <sup>2</sup>	candela/m <sup>2</sup>	0.2919	foot-Lamberts	fl
<b>FORCE and PRESSURE or STRESS</b>				
N	newtons	0.225	poundforce	lbf
kPa	kilopascals	0.145	poundforce per square inch	lbf/in <sup>2</sup>
*SI is the symbol for the International System of Units. (Adapted from FHWA report template, Revised March 2003)				



## List of Abbreviations and Acronyms

AASHTO	American Association of State Highway and Transportation Officials
AMPT	Asphalt Mixture Performance Tester
BBR	Bending Beam Rheometer, refers to AASHTO TP-125
CT Index	Cracking Tolerance Index
FHWA	Federal Highway Administration
HMA	Hot Mix Asphalt
IDEAL-CT	Indirect Tension Asphalt Cracking Test, refers to ASTM D8225
LCCA	Life-Cycle Cost Analysis
MEPDG	Mechanistic-Empirical Pavement Design Guide (Software called AASHTOWare Pavement ME®)
MnROAD	Minnesota's Cold Weather Pavement Testing Facility
NCHRP	National Cooperative Highway Research Program
PG	Performance Grade
RAP	Reclaimed Asphalt Pavement
SCB-IFIT	Semi-Circular Bending Illinois Flexibility Index Test
UDOT	Utah Department of Transportation
U of U	University of Utah
VFA	Voids Filled with Asphalt
VMA	Voids in the Mineral Aggregate

# Executive Summary

This research developed a practical method to relate UDOT's existing material tests for asphalt mixtures, including the Bending Beam Rheometer (BBR) for low-temperature behavior and IDEAL-CT for intermediate-temperature cracking, to the dynamic modulus ( $E^*$ ) master curve required for Level 1 inputs in AASHTOWare Pavement ME®. The proposed approach allows for accurate prediction of  $E^*$  using simplified testing, eliminating the need for extensive dynamic modulus testing while preserving reliability. Thanks to the advances from this work, it is now possible to use materials with the same properties during all aspects of pavement design and construction, thus allowing for life-cycle cost analysis.

Testing of different asphalt mixtures revealed a wide variability in expected performance among mixtures even though they were designed with identical specifications, underscoring the value of performance-based evaluations. Incorporating BBR-measured low-temperature data into dynamic modulus master curve showed that models relying solely on volumetric properties may miss critical mixture interactions. While actual measurements of the limiting value of the dynamic modulus proved elusive, models using measured low-temperature  $E^*_{\max}$  values provided improved insights over generalized volumetric relations like the Hirsch model.

Validation of this work using the AASHTOWare Pavement ME® software showed no significant difference in the pavement design when using the simplified method proposed by this work; thus, confirming its suitability for practical implementation.

Key benefits of this work include: (1) direct linkage between material properties and pavement design for improved life-cycle cost analysis, (2) use of project-specific data instead of national averages, and (3) a significant reduction in testing time requirements from weeks to days and the corresponding decrease in laboratory effort.

Overall, this study offers a streamlined, accurate, and efficient process for estimating dynamic modulus master curves in an improved pavement design process.

# Chapter 1.0 Introduction

## 1.1 Background

The durability and long-term performance of asphalt pavements are influenced directly by the mechanical characteristics of the asphalt mixture. Designing pavements using a mechanistic characterization process requires many material properties, including the relation between load and deformation of the material at different loading frequencies and temperatures. The dynamic modulus of asphalt concrete provides such a relation, and it is used in the mechanistic-empirical pavement design guide process as input to the AASHTOWare Pavement ME® design software. A dynamic modulus master curve outlines the viscoelastic material behavior as a function of temperature and loading duration or frequency [1]. AASHTO R84-17, also known as “Standard Practice for Developing Dynamic Modulus Master Curves for Asphalt Mixtures Using the Asphalt Mixture Performance Tester,” provides details on testing and analysis methods for developing a dynamic modulus master curve for asphalt mixtures. The process starts by measuring the dynamic modulus of asphalt mixtures at different loading frequencies and at specific temperatures. The results from the different temperatures are combined into a dynamic modulus master curve. The construction of a master curve follows the time-temperature superposition principle, involving overlaying dynamic modulus and phase angle values from test data obtained at various temperatures and frequencies.

The use of the dynamic modulus of asphalt mixtures as an input parameter to predict flexible pavement performance assumes that the material tested and used as input in the pavement design process is the same material used to build the pavement. However, due to the complexities of measuring the dynamic modulus, accurate material inputs for the design process are not always available. This leads to using average or default values that may not accurately represent what is used in the field (i.e., Level 3 inputs). Consequently, this practice can result in overestimation or underestimation of rutting, fatigue, and thermal cracking in pavement sections by the AASHTOWare

Pavement ME® process. As a result, opportunities for cost optimization are missed when selecting suitable asphalt mixtures for specific pavement projects [2].

Even if the same materials available during the design process were available for construction, the cost, time, and effort constraints required to perform the dynamic modulus test limit its use. Furthermore, the machine needed to run the tests, namely the Asphalt Mixture Performance Tester (AMPT), is not readily available in all laboratories. At the same time, routine tests during the asphalt mixture design process, such as the IDEAL-CT, the SCB-IFIT, or the Bending Beam Rheometer for mixtures, are not currently used as input to the pavement structural design process. This work seeks to approximate the dynamic modulus master curve of asphalt mixtures by incorporating measured values from the single-value tests used during mix design. In addition to benefiting from providing site-specific material inputs for pavement design, these simpler testing methods can decrease the gap between laboratory testing predictions and field performance, resulting in better pavement designs.

## 1.2 Objectives

The overall objective of this research series is to develop a relationship between material tests that are currently being used by UDOT (Bending Beam Rheometer for mixtures at low temperatures and IDEAL-CT at intermediate temperatures), and the dynamic modulus,  $E^*$ , master curve values used as input to the pavement design software (Level 1 in AASHTOWare Pavement ME®). Such a relation is expected to allow for selection of a dynamic modulus,  $E^*$ , master curve that is directly related to the asphalt mixture used in the pavement while significantly simplifying testing. **This in no way implies that direct measurements of the dynamic modulus master curve are not desired; it means that the values can be approximated with less effort using the developed relations.** This capability will have several benefits that include: 1- directly relate materials properties to pavement design allowing for life-cycle cost analysis, 2-use input values that actually relate to the material properties used in construction instead of using national averages, and 3-simplify the required testing from weeks to days. To accomplish this objective, a multi-phase approach was proposed:

Phase I was used to prove the feasibility of this approach [3]; Phase II was used to develop relations at intermediate temperatures [4]; Phase III verifies the relation with other types (i.e., families) of mixtures and incorporates data at low temperatures to the dynamic modulus master curve.

The specific objectives of Phase III are:

- Expand the relations that predict the dynamic modulus master curve from IDEAL-CT data to incorporate different types of asphalt mixtures. Two mixtures were obtained from MnROAD to expand the relations.
- Incorporate low-temperature properties on all 11 mixtures (nine from Phase II and two from this phase) into the dynamic modulus master curve to relate BBR results to the pavement design. These results will allow the development of a master curve incorporating measured values at low temperatures instead of using values from a Hirsch model as it is currently done.
- Develop a relation between single-point tests and the time-temperature shift factor. The time-temperature shift factor will then be incorporated into the dynamic modulus master curve equation so that the dynamic modulus at any frequency and time can be predicted and used as input to AASHTOWare Pavement ME®.
- Create a full master curve and compare measured and predicted values. Quantify the prediction error compared to the equations developed in Phase II.
- Create a process to develop a dynamic modulus of asphalt mixtures based on relations developed that allow for direct input to AASHTOWare Pavement ME®.

### **1.3 Scope**

Asphalt mixtures have been obtained from different sources that include seven plant-produced mixtures from the state of Utah, two plant-produced mixtures from the state of Minnesota, and two laboratory-produced mixtures prepared using binders developed based on specifications for Idaho and Nevada.

Mixes #1 to #6 were plant-produced mixtures used by UDOT as surface materials, Mix #7 was a plant-produced mixture with different binder grade used as a road base, Mixes #8 and #9 were laboratory-prepared mixes created at the University of Utah Materials and Pavement Laboratory using binders formulated based on specifications for Nevada and Idaho, respectively. Finally, Mixes #10 and #11 were plant-produced mixtures obtained from the Minnesota Department of Transportation and correspond to Cells 18 and 21 from their MnROAD research program. All of the samples were tested in intermediate and low-temperature conditions following the procedures of four different tests: the IDEAL-CT Index and SCB-IFIT at an intermediate temperature of 25 °C, the Asphalt Mixture Performance Tester (AMPT) at 0.01, 0.1, 1, and 10 Hz. frequencies and temperatures of 4 °C, 25 °C and 40 °C, and the Bending Beam Rheometer (BBR) at temperatures ranging from 0 °C to -24 °C. All samples were prepared using the Superpave gyratory compactor (SGC) at the University of Utah with a target air void of 7.0% ± 0.5.

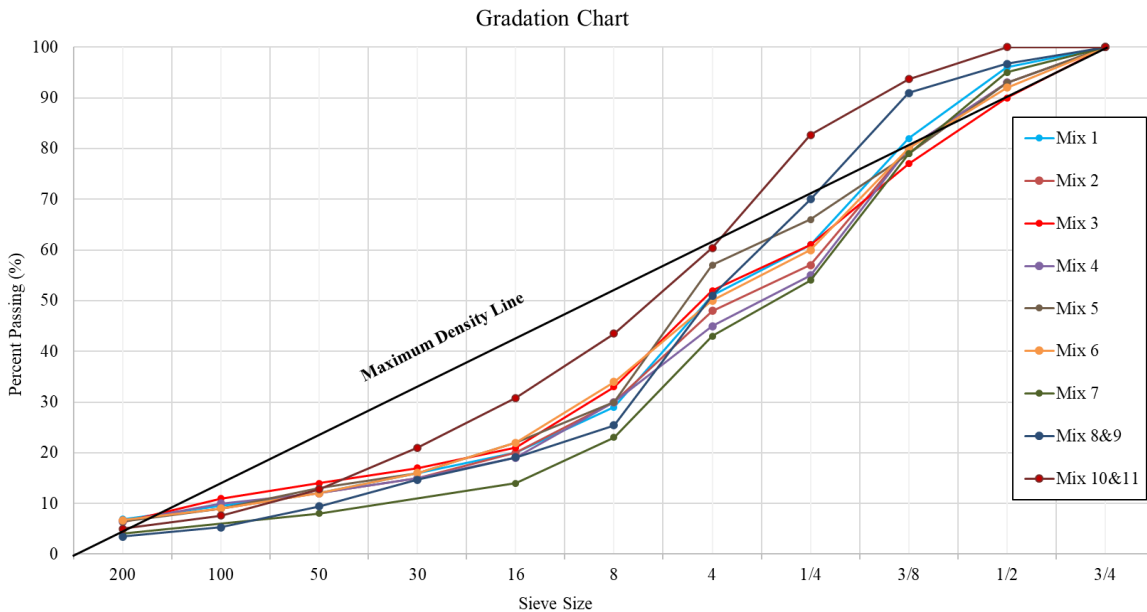
The first six mixtures obtained during Phase I (Report UT-22.18) [3] were surface layer designs with PG 64-34 asphalt binder and 25% Reclaimed Asphalt Pavement (RAP). Mix #7 is a base layer obtained during Phase II (Report UT-24.02) [4] and prepared with PG 58-28 asphalt binder. Mixes #8 and #9 are laboratory-produced with PG 64-34 binder formulated following different specifications for Nevada and Idaho, respectively. Mixes #10 and #11 were designed to be placed on the westbound lanes of Interstate 94 in Albertville, MN. Mix #10 uses an unmodified PG 64S-22 binder to increase the low-temperature cracking potential and 20% RAP. Mix #11 utilizes a PG 58H-34 binder with 20% RAP. Table 1 shows the description of each of the mixes used.

**Table 1 - Description of Mixtures**

Lab ID	Origin Pin	Location	Binder Grade	Asphalt Binder Content (%)	Virgin Binder of the Mix (%)	RAP Binder of the Mix (%)	RAP by Weight of Mixture (%)
Mix #1	17230	SR-10	PG 64-34	5.59	4.22	1.38	25.00
Mix #2	17505	SR- 198	PG 64-34	4.90	3.90	1.00	25.00
Mix #3	17307	SR-150	PG 64-34	5.20	4.05	1.15	25.00
Mix #4	16534	SR-90	PG 64-34	5.00	3.75	1.25	23.00
Mix #5	17305	SR-302	PG 64-34	4.91	3.78	1.13	25.00
Mix #6	15252	SR-112	PG 64-34	5.00	3.80	1.20	25.00
Mix #7	15688	Base	PG 58-28	4.90	3.78	1.12	--
Mix #8	Peak	N/A	Peak 64-34	5.30	4.90	0.40	10.00
Mix #9	Paramt	N/A	Par 64-28N	5.30	4.90	0.40	10.00
Mix #10	Cell 18	Westbound I-94	PG 64S-22	5.43	4.20	1.23	20.00
Mix #11	Cell 21	Westbound I-94	PG 58H-34	5.38	4.15	1.23	20.00

### 1.3.1 Mixture Gradations

All plant-produced mixtures except Mix #7 were designed as 12.5-mm surface mixtures. Laboratory-produced Mixes #8 and #9 are intended to represent surface mixtures in terms of gradation. The gradations based on standard U.S. sieve sizes for all mixtures are shown in Figure 1.

**Figure 1 - Gradation Chart of all Mixtures.**

## **1.4 Outline of Report**

This report presents the research results conducted on 11 asphalt mixes. The introductory chapter provides the background, objectives, and scope of the study, detailing the mixture gradation, location, and some relevant properties. The research methodology covers various testing procedures such as the IDEAL-CT, the Bending Beam Rheometer, Illinois Flexibility Index, and Asphalt Mixture Performance Test. The subsequent chapter on data testing and analysis includes detailed procedures and findings from the Indirect Tension Asphalt Cracking Test (IDEAL-CT), Bending Beam Rheometer tests, and the Semi-Circular Bending Illinois Flexibility Index Test (SCB-IFIT) and the Asphalt Mixtures Performance Tester (AMPT). The report also includes a summary of the findings, a thorough analysis of the test data, and references to relevant literature.



# **Chapter 2.0 Research Methodology**

## **2.1 Overview**

This chapter offers an overview of the research and methodology used in this study, presenting a concise summary and outline of the suggested approach. The following sections cover the methodology associated with the IDEAL-CT Index, Bending Beam Rheometer (BBR), SCB-IFIT, and Asphalt Mixture Performance Tester (AMPT). This is included for completeness as detailed descriptions have been included in previous reports.

## **2.2 IDEAL-CT and Cracking Tolerance Index**

Predicting cracking and rutting in asphalt pavements has always been a challenge in pavement engineering. The introduction of the IDEAL-CT test aims to predict asphalt pavement's resistance to cracking through the Cracking and Tolerance Index (CT-index). Although semi-empirical in nature, this index is said to indicate whether a pavement is more resistant to cracking; a higher CT Index signifies greater resistance. The IDEAL-CT test has gained prominence due to its simplicity, making it a valuable tool in materials and pavement engineering. This test is similar to the standard indirect tensile strength tests and involves applying a vertical monotonic load to a cylindrical specimen at a constant head displacement rate of 50 mm/min. The test concludes when the load drops to 0.1 kN [5], [6]. Crosshead displacement is continuously measured and recorded throughout the test, with data analysis based on a load versus displacement curve. The CT Index is derived from the total fracture energy and the slope of the post-peak curve at a 25% decrease from the peak load.

### **2.2.1 Test Procedure**

The hot-mix asphalt was transported in metal buckets to the Pavement and Materials Laboratory at the University of Utah. The mixes were heated overnight to 120 °C with the lid closed to prevent aging. After reaching a pliable state, each sample

replicate was divided using quartering methods. The hot mix was weighed to achieve the target air voids at specified heights based on the maximum specific gravity (G<sub>mm</sub>). The mix was heated to the designated compaction temperature and compacted using the Superpave Gyratory Compactor (SGC), following AASHTO T312 procedures: Standard Method of Test for Preparing and Determining the Density of Asphalt Mixtures using the Superpave Gyratory Compactor.

Each sample was compacted to a height of 62 mm and a diameter of 150 mm, after which the air voids for each sample were determined following the guidelines in AASHTO T269: Percent Air Voids in Compacted Dense and Open Asphalt Mixtures. The number of gyrations required for compaction and the resulting air voids were recorded for each sample.

Testing was done based on ASTM D8225: Standard Test Method for Determination of Cracking Tolerance Index of Asphalt Mixture Using the Indirect Tensile Cracking Test at Intermediate Temperature. The samples were tested within 8 to 24 hours after compaction to ensure consistency. Each sample was conditioned for 2 hours at 25 °C and at constant humidity, after which the test was carried out.

The testing equipment digitally collected load-displacement data and determined the cracking tolerance (CT) index for each sample by calculating the area under the curve of the load-displacement curve and the post-peak slope generated by the test. This process resulted in about 4 values per mix and about 44 values for all mixes. The CT Index is calculated based on Equation 1.

$$CT_{index} = \frac{G_f}{|m_{75}|} \times \left( \frac{175}{D} \times \frac{t}{62} \times 10^6 \right) \quad \text{Equation 1}$$

Where:

$G_f$  = The energy required to create a unit surface area of a crack, Joules/m<sup>2</sup>.

$D$  = Specimen diameter, mm.

$t$  = Specimen's thickness, mm.

$$|m_{75}| = \left| \frac{P_{85} - P_{65}}{l_{85} - l_{65}} \right| = \text{the value of the slope defined between the 85\% and 65\%}$$

peak load point of the load-displacement curve after the peak, N/m, and

$l_{75}$  =  $l_{75}$  deformation tolerance at 75 percent maximum load, mm.

Generally, the higher the  $G_f$ , the better the cracking resistance of asphalt mixtures is expected. The stiffer the mix, the faster the cracking rate, the faster the load decreases, the higher the value of the slope  $|m_{75}|$ , and the lower the cracking resistance. Mixes with higher strain tolerance have stronger cracking resistance than those with lower strain tolerance [6].

### 2.2.2 Quality Control

Before the analysis, a quality control procedure was implemented to ensure the data's representativeness. In the case of the IDEAL-CT, four specimens underwent testing; the average and the standard deviation of the CT Index were calculated. Instances where the standard deviation exceeded 25% of the mean (indicating a coefficient of variation greater than 25%) prompted an outlier analysis. If the highest value lay beyond the interquartile range of  $Q3 + 1.5 \cdot IQR$ , it was flagged as an outlier and excluded from further analysis. Each mix was evaluated with no fewer than three data points analyzed.

## 2.3 Bending Beam Rheometer (BBR)

Cold regions face deterioration in asphalt pavements caused primarily by distress due to thermal cracking. This occurs when the asphalt mixture is brittle and the Hot Mix Asphalt (HMA) surface contracts due to low temperatures, resulting in stress buildup. To prevent thermal cracking, it is desirable to select materials with the ability to relax the thermal stresses [7]. While selecting the proper asphalt binder is important, brittle mixtures generally result from the design with an emphasis on rut resistance and the addition of reclaimed asphalt pavement (RAP) [8].

Previous work at the University of Utah [9], [13] demonstrated that the BBR test can assess the rheological properties of asphalt mixtures. This helps understand their

creep stiffness and relaxation properties to predict the possibility of thermal cracking in asphalt pavements. With a sample size of 12.7 mm x 6.35 mm x 127 mm (width x thickness x length), the study conducted by Romero et al. showed that the beams are a representative volume element, and the effect of the size of the beam compared with the aggregate size does not introduce variability in the results [9]. It is convenient to have a small sample size, as it allows enough samples to be obtained from field cores or laboratory-compacted specimen.

AASHTO TP 125 (2016) covers the procedure for determining the flexural-creep stiffness or compliance and m-value of asphalt mixtures using a Bending Beam Rheometer (BBR). The flexural creep stiffness or flexural creep compliance obtained from this test describes the low-temperature stress-strain-time behavior of asphalt mixtures at the test temperature within the range of linear viscoelastic response. These properties are used as performance-based criteria to accurately determine the rheological properties of asphalt mixtures, especially in cold regions. The BBR output reports the creep modulus and m-value of the beams at 60 seconds.

### **2.3.1 Test Procedures**

The Bending Beam Rheometer test samples were cut from laboratory-compacted Superpave gyratory compactor specimens at the University of Utah, targeting an air void of  $7.0\% \pm 0.5$ . The specimens were cut following the AASHTO TP 125-22 standard to the required dimensions. All the procedures for making the asphalt mixture beams for BBR testing are described in the UDOT report from a previous study: Report No. UT-16.09 [9].

Before testing, each sample is soaked in the bath for 60 minutes to ensure the entire beam reaches the test temperature. Each test produces a series of data over time, including force and deflection as functions of time. The device measures and records the deformation response of the beam to the applied load, and these values are then used to calculate Creep stiffness and m-value at specified times (usually 60 seconds). Specific details and requirements for the BBR test procedure can be found in the AASHTO TP 125-22 standard.

### **2.3.2 Quality Control**

This study tested the 11 mixtures previously described. For each mixture, 15 specimens were cut from the Superpave Gyratory Compactor sample. These specimens were then subjected to the Bending Beam Rheometer test to evaluate their low-temperature performance, varying the temperature from -24 °C to 0 °C at 6-degree intervals. Following established protocols, a trimmed-mean method was used when the standard deviation of the creep stiffness at 60 seconds exceeded 25% of the mean. The trimmed mean consisted of dropping the high and low values from the analysis. At least eight data values for each condition were used to determine the mean in all cases.

## **2.4 Illinois Flexibility Index (SCB-IFIT)**

The SCB-IFIT test was developed by the Illinois Center for Transportation to predict the cracking of asphalt materials with RAP contents of up to 50%. UDOT originally selected this test, but it has since fallen out of favor. This study used this test since it incorporates fracture mechanical principles that might better relate to cracking. Given the limited material available, only Mixes #1 to #6, #10, and #11 were tested in SCB-IFIT.

### **2.4.1 Test Procedure**

The SCB-IFIT, or Illinois Flexibility Index test, adhered to the guidelines outlined in AASHTO TP 124 (Illinois version). Sample preparation followed the same procedure described in Section 2.2.1. Each sample was compacted to a height of 50 mm and a diameter of 150 mm at the target air voids. A half circle was made by cutting the SGC specimens across their diameter. Across the center of the flat side, a  $15 \pm 1$  mm deep notch was cut. Measurements were taken and recorded for use in calculations. All four notched, half rounds were then dried and incubated in conditioned air to 25 °C in preparation for testing in less than 24 hours. Employing the same apparatus as the IDEAL-CT test, the SCB-IFIT test varied in specimen configuration, utilizing the three-point bending principle. Maintaining a consistent head displacement rate of 50 mm/min, the parameters of the load-displacement curve were analyzed to ascertain the Flexibility

Index value. This value is computed by dividing the fracture energy by the absolute value of the post-peak load slope, subsequently multiplied by a conversion factor. This is shown in Equation 2.

$$FI = \frac{Gf}{|m|} \times A \quad \text{Equation 2}$$

In this equation,  $Gf$  represents the fracture energy ( $\text{J/m}^2$ ) obtained by dividing the work of fracture (the area under the load-displacement curve) by the ligament area. The term  $|m|$  refers to the absolute value of the post-peak load slope. Additionally, factor  $A$  is equal to 0.01. To calculate the ligament area, which is the cross-sectional area of the specimen where the crack propagates, one can multiply the ligament width (the thickness of the test specimen) by the ligament length.

## 2.5 Asphalt Mixture Performance Tester (AMPT)

The Asphalt Mixture Performance Tester (AMPT) is used to determine the dynamic modulus ( $E^*$ ) of asphalt mixtures across varying temperatures and loading conditions as part of the process in the Mechanistic-Empirical Pavement Design Guide (MEPDG). The dynamic modulus is predicted at all temperature and loading rates through the master curve using the time-temperature superposition principle. The master curve illustrates the time-dependent behavior of the material as a function of the temperature and loading duration or frequency. The master curve is created by overlaying the dynamic modulus and phase angle values derived from test data obtained at different temperatures and frequencies [10], [11]. AASHTO R84 outlines the procedure for creating dynamic modulus master curves for asphalt mixtures using the AMPT.

### 2.5.1 Dynamic Modulus Master Curve

To obtain the dynamic modulus of compacted asphalt mixtures at any temperature and loading frequency, the data collected from the AMPT is fitted into Equation 3, as outlined in AASHTO R84.

$$\log|E^*| = \delta + \frac{Max - \delta}{1 + e^{\beta + \gamma \log \omega_r}} \quad \text{Equation 3}$$

This equation predicts the dynamic modulus,  $E^*$ , as a function of reduced frequency,  $\omega_r$ , based on four fitted parameters: delta, beta, gamma, and Max. Max represents the limiting maximum value of the dynamic modulus. It is determined based on a Hirsch Model incorporating Voids in the Mineral Aggregate, VMA, and Voids Filled with Asphalt, VFA, from the asphalt mixture design; it is not a measured or fitted parameter. Similarly, the other three parameters ( $\delta$ ,  $\beta$ , and  $\gamma$ ) define the shape of the curve and are determined based on a least squares' minimization procedure.

The reduced frequency is obtained through the time-temperature shift factor. The shift factor is determined using the test temperature (T), the reference temperature ( $T_r$ ), and the activation energy ( $\Delta E_a$ ) based on Equation 4.

$$\log(\omega_r) = \log(\omega) + \frac{\Delta E_a}{19.14714} \left( \frac{1}{T} - \frac{1}{T_r} \right) \quad \text{Equation 4}$$

## 2.6 Relation Between Single Point/Index Tests and Dynamic Modulus

In this third phase of the study, the primary aim is to validate the relationship between various tests discussed in this chapter and the dynamic modulus of asphalt mixtures. The theoretical results from Phase I [3] were validated in Phase II [4] by measuring dynamic modulus and cracking tolerance index values across nine different mixtures. Phase III builds on this by including two additional mixes and incorporating the BBR test into the analysis. Although the mode and rate of loading in each test differ, Phase II demonstrated that relationships exist between different test modes. Based on simplified assumptions, it was hypothesized that the response of a material during a mechanical test represents the transfer of energy from one form to another, potentially resulting in new surfaces, material flow, or heat. Assuming minimal system losses, a relationship in Equation 5 was proposed between the results of IDEAL-CT tests and the dynamic modulus [3].

$$\Delta W \propto \frac{\sin(2\delta)}{E^*}$$

**Equation 5**

Here,  $\Delta W$  represents the area under the load-displacement curve from IDEAL-CT tests while  $E^*$  and  $\delta$  are the dynamic modulus and phase angle from the AMPT tests, respectively. This suggests that IDEAL-CT results may inversely relate to the parameters of the dynamic modulus master curve [4]. This hypothesis was tested with positive results in both Phase I and Phase II. Incorporating creep stiffness from the BBR at low temperatures is the subject of research during this phase.



## Chapter 3.0 Data Testing and Analysis

The results of the testing and the analysis of the data are presented in this chapter.

### 3.1 IDEAL-CT Testing and Data Analysis

Eleven mixtures were tested for this project, revealing varying CT Index values. Figure 2 presents the CT Index of various samples with the coefficient of variations and their corresponding fracture energy. The CT-Index value ranged from a high of almost 120 to a low of over 20. The fracture energy ranged from a high of 9 kJ/m<sup>2</sup> to a low of less than 5 kJ/m<sup>2</sup>. The varied results in Mixes #1 to #6 demonstrate that the mixtures yielded different performance outcomes despite being designed for the same environment, with the same specifications and the same binder grades.

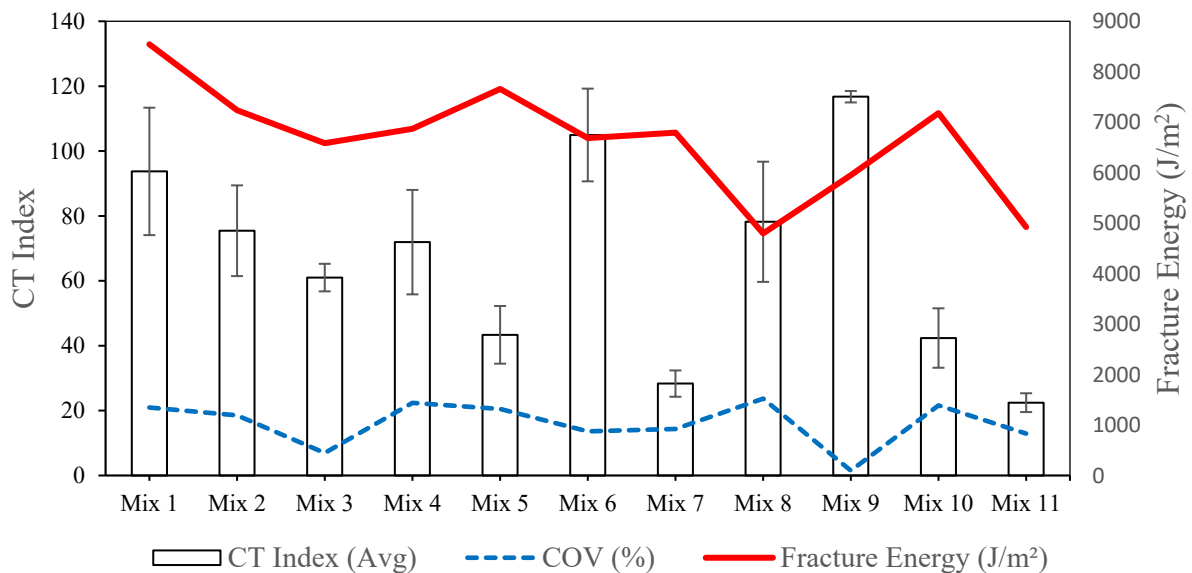


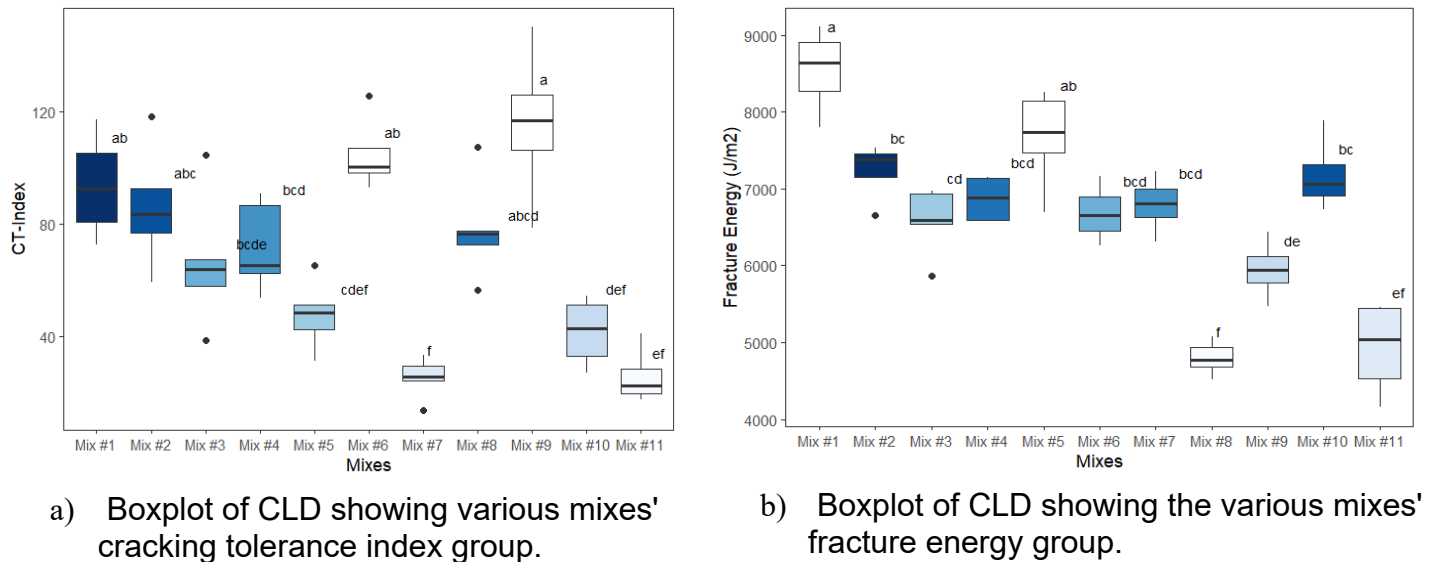
**Figure 2 - Graphical Representation of Mixes' CT Index and Fracture Energy.**

Statistical analyses were further conducted to explore the differences in properties among different mixes. The properties considered included the cracking tolerance index and the fracture energy, all assessed at room temperature. Table 2 shows the Pearson correlation between variables.

**Table 2 - Pearson Correlation Between Variables.**

	<i>CT Index</i>	<i>Fracture Energy(J/m<sup>2</sup>)</i>	<i>Post Peak Slope</i>	<i>Max Load (kN)</i>	<i>Air Voids</i>
CT Index	1.00				
Fracture Energy (J/m <sup>2</sup> )	0.32	1.00			
Post Peak Slope	-0.64	0.38	1.00		
Max Load (kN)	-0.34	0.69	0.92	1.00	
Air Voids	-0.29	0.31	0.73	0.70	1.00

A Tukey's test analysis was conducted to provide pairwise comparisons between the means of different mixes for CT Index and Fracture Energy based on a 95% family-wise confidence level. Figure 3 shows a boxplot of the Compact Letter Display (CLD) statistical method to clarify the Tukey tests' output. The boxplot is categorized with the same letter for each mixture in that the mean is not statistically different from another one. Mixtures in the same group would be expected to have similar performance.

**Figure 3 - Compact Letter Display Boxplot for Grouping Mixes with Similar IDEAL-CT Index Results.**

From Figure 3, it can be observed that Mixes #1, #2, #6, #8, and #9 belong to the same high CT Index value and are expected to perform well in fatigue cracking. Likewise, Mixes #5, #7, #10, and #11 belong to the same low CT Index value and are not expected to perform well. Looking at fracture energy, it can be seen that Mixes #1 and #5 belong in the same high fracture energy group, while Mixes #8 and #11 belong

in the same low fracture energy group. These different groups demonstrate that this study incorporates a variety of mixtures with different expected performance.

## 3.2 Bending Beam Rheometer

Eleven mixtures were tested at low temperatures, revealing varying stiffness and temperature susceptibility levels.

### 3.2.1 BBR Data Visualization

The results of the BBR test provided valuable insights into the expected performance characteristics of each mixture at low temperatures. This section addresses the statistical analyses performed to identify significant variations in the results and the sources of variation. Standard deviation and Coefficient of Variation (COV) were used to quantify the distance of the raw data point from the mean and set a threshold for outliers. Artificial outliers were removed to visualize the average stiffness and m-value of the BBR in Figure 4 and Figure 5. The descriptive statistics with average, standard deviation, and covariance are shown in Table 3. For all mixtures, stiffness decreased as temperature increased, which was expected. Conversely, the m-value increased with the rise in temperature.

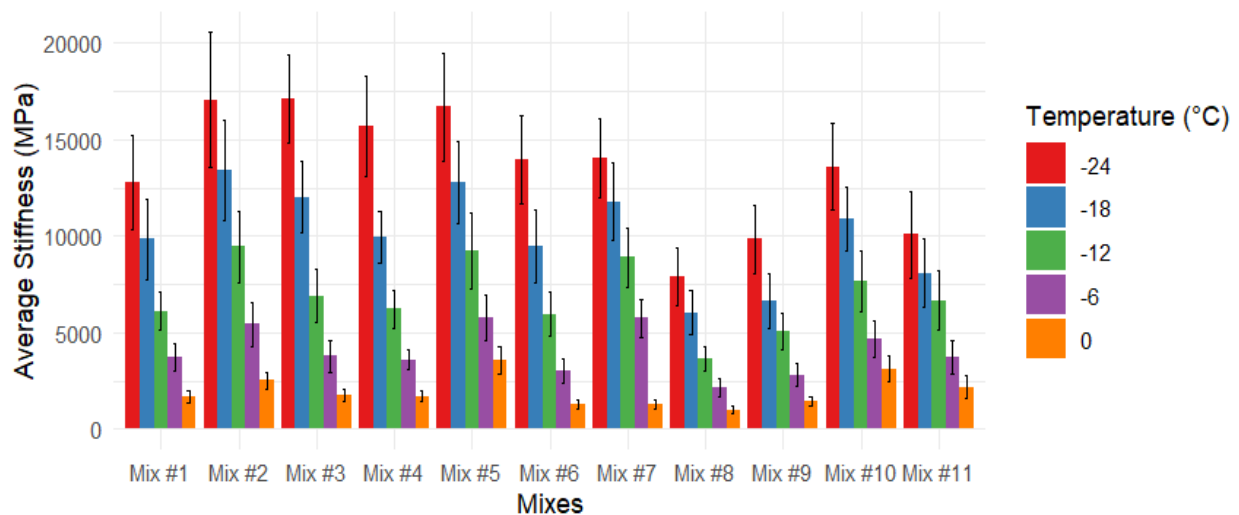
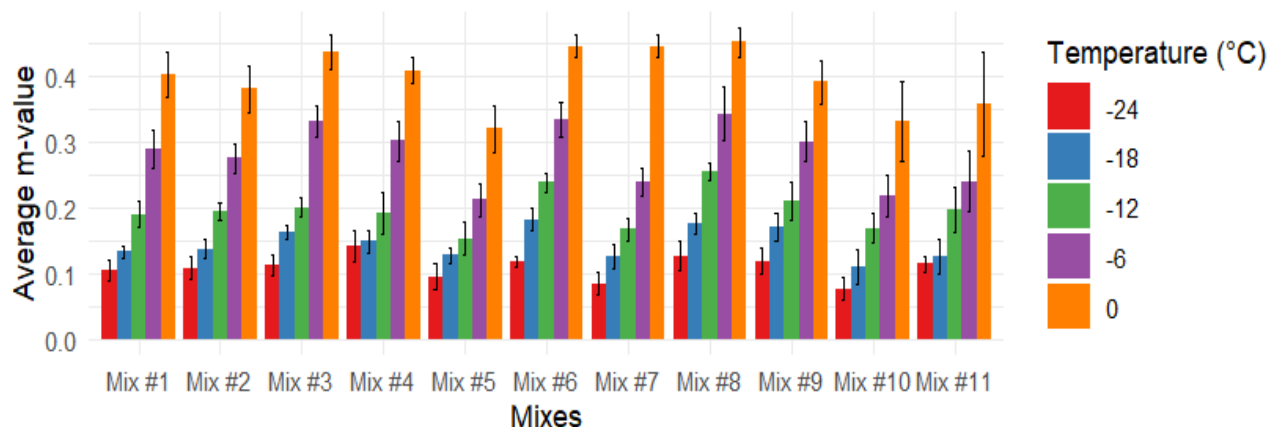


Figure 4 - Average Stiffness at 60 s.



**Figure 5 - Average m-value at 60 s.**

**Table 3 - Descriptive Statistics: Average, Standard Deviation, and Coefficient of Variation (COV) for Stiffness and m-value.**

Mix	Temp (°C)	Average Stiffness_60s (MPa)	Std. Dev Stiffness	COV Stiffness	Average m-value	Std. Dev m-value	COV m-value
Mix #1	0	1669.40	319.56	0.19	0.40	0.03	0.08
Mix #1	-6	3737.14	719.78	0.19	0.29	0.03	0.10
Mix #1	-12	6116.75	995.96	0.16	0.19	0.02	0.10
Mix #1	-18	9858.76	2092.02	0.21	0.13	0.01	0.07
Mix #1	-24	12766.39	2443.91	0.19	0.10	0.02	0.15
Mix #2	0	2537.88	423.13	0.17	0.38	0.04	0.09
Mix #2	-6	5427.12	1114.41	0.21	0.27	0.02	0.08
Mix #2	-12	9443.86	1841.59	0.07	0.19	0.01	0.07
Mix #2	-18	13402.62	2566.69	0.19	0.14	0.01	0.10
Mix #2	-24	17065.93	3525.27	0.21	0.11	0.02	0.16
Mix #3	0	1770.13	317.63	0.18	0.44	0.03	0.06
Mix #3	-6	3797.41	811.88	0.21	0.33	0.02	0.07
Mix #3	-12	6907.53	1381.60	0.07	0.20	0.01	0.07
Mix #3	-18	12029.33	1875.92	0.16	0.16	0.01	0.07
Mix #3	-24	17111.81	2272.89	0.13	0.11	0.02	0.14
Mix #4	0	1725.13	281.04	0.16	0.41	0.02	0.05
Mix #4	-6	3604.78	504.64	0.14	0.30	0.03	0.10
Mix #4	-12	6215.04	958.60	0.17	0.19	0.03	0.17
Mix #4	-18	9918.78	1341.94	0.14	0.15	0.02	0.12
Mix #4	-24	15726.35	2599.10	0.17	0.14	0.02	0.17
Mix #5	0	3576.95	726.62	0.20	0.32	0.04	0.11
Mix #5	-6	5781.64	1161.22	0.20	0.21	0.03	0.12
Mix #5	-12	9256.74	1955.15	0.17	0.15	0.03	0.17
Mix #5	-18	12767.46	2102.55	0.16	0.13	0.01	0.09
Mix #5	-24	16683.33	2792.19	0.17	0.09	0.02	0.21
Mix #6	0	1286.62	251.73	0.20	0.45	0.02	0.04
Mix #6	-6	3018.76	647.75	0.21	0.33	0.03	0.08

Mix #6	-12	5963.56	1149.10	0.06	0.24	0.01	0.06
Mix #6	-18	9448.60	1890.85	0.20	0.18	0.02	0.10
Mix #6	-24	13961.24	2288.01	0.16	0.12	0.01	0.07
Mix #7	0	1286.62	251.73	0.20	0.45	0.02	0.04
Mix #7	-6	5767.31	989.05	0.17	0.24	0.02	0.09
Mix #7	-12	8895.19	1503.26	0.17	0.17	0.02	0.10
Mix #7	-18	11775.81	1990.25	0.17	0.13	0.02	0.15
Mix #7	-24	14045.91	2065.53	0.15	0.08	0.02	0.21
Mix #8	0	997.01	188.82	0.19	0.45	0.02	0.05
Mix #8	-6	2168.63	474.46	0.22	0.34	0.04	0.12
Mix #8	-12	3669.96	605.80	0.17	0.25	0.01	0.05
Mix #8	-18	6031.07	1149.96	0.19	0.18	0.02	0.09
Mix #8	-24	7894.96	1484.18	0.19	0.13	0.02	0.18
Mix #9	0	1448.34	231.10	0.16	0.39	0.03	0.08
Mix #9	-6	2827.49	595.99	0.21	0.30	0.03	0.10
Mix #9	-12	5073.55	956.58	0.19	0.21	0.03	0.14
Mix #9	-18	6636.61	1425.76	0.21	0.17	0.02	0.13
Mix #9	-24	9855.32	1777.86	0.18	0.12	0.02	0.17
Mix #10	0	3131.06	650.64	0.21	0.33	0.06	0.18
Mix #10	-6	4682.07	912.91	0.19	0.22	0.03	0.15
Mix #10	-12	7656.37	1572.46	0.21	0.17	0.02	0.13
Mix #10	-18	10915.26	1638.05	0.15	0.11	0.03	0.24
Mix #10	-24	13600.80	2237.53	0.16	0.08	0.02	0.22
Mix #11	0	2197.55	572.03	0.26	0.36	0.08	0.22
Mix #11	-6	3715.43	872.74	0.23	0.24	0.05	0.20
Mix #11	-12	6672.91	1559.22	0.23	0.20	0.04	0.18
Mix #11	-18	8073.60	1759.39	0.22	0.13	0.03	0.21
Mix #11	-24	10083.63	2235.20	0.22	0.11	0.01	0.11

### 3.2.2 BBR Data Analysis

Figure 6 to Figure 10 show a boxplot of the Compact Letter Display (CLD) statistical method to clarify the output of the ANOVA and Tukey tests. The boxplot is categorized with the same letter for each mixture, with the mean not statistically different from the other.

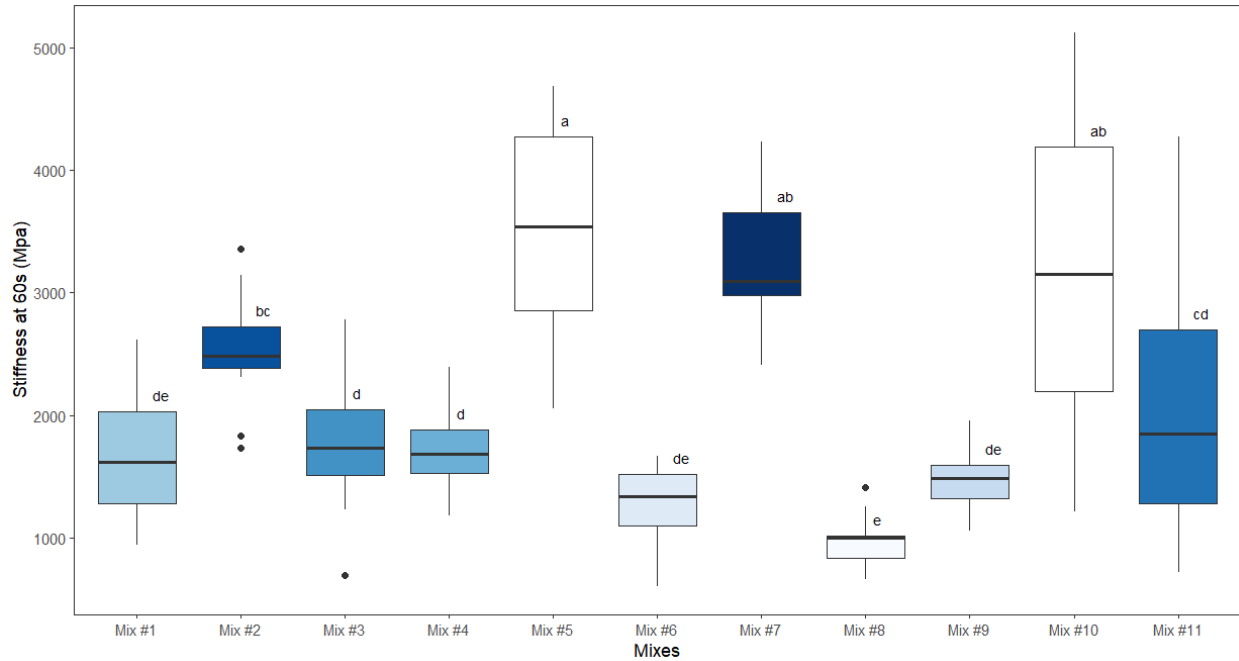


**Figure 6 – Compact Letter Display Boxplot for Creep Stiffness at 0 °C**

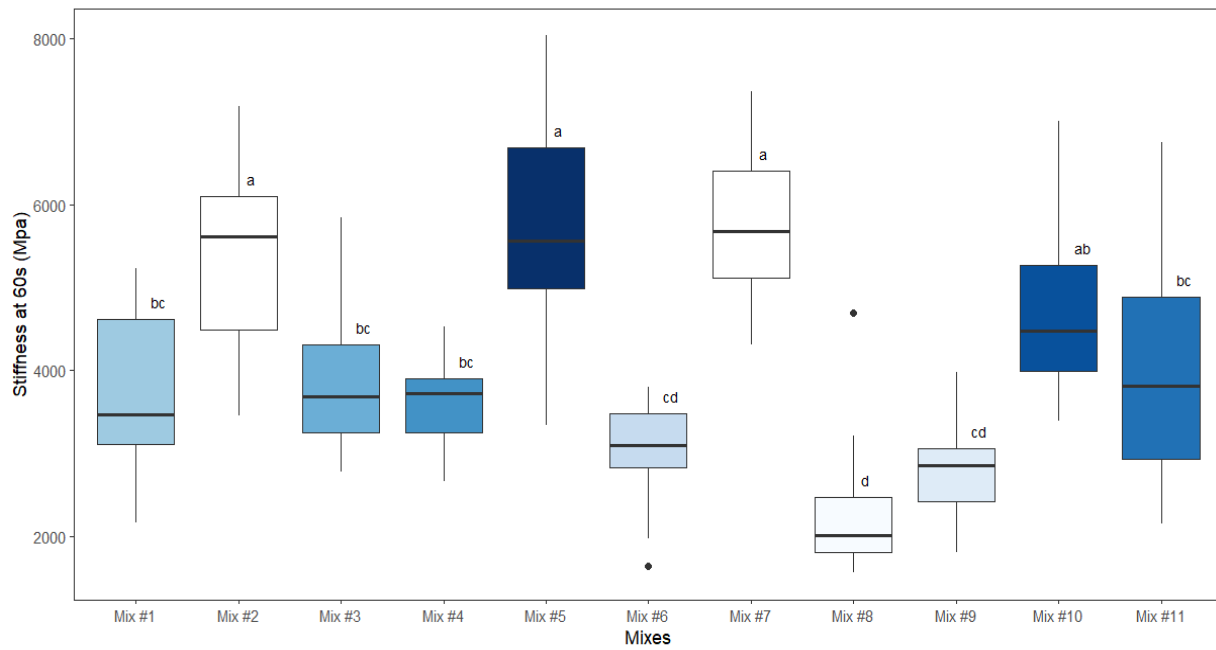


**Figure 7 – Compact Letter Display Boxplot for Creep Stiffness at -6 °C**

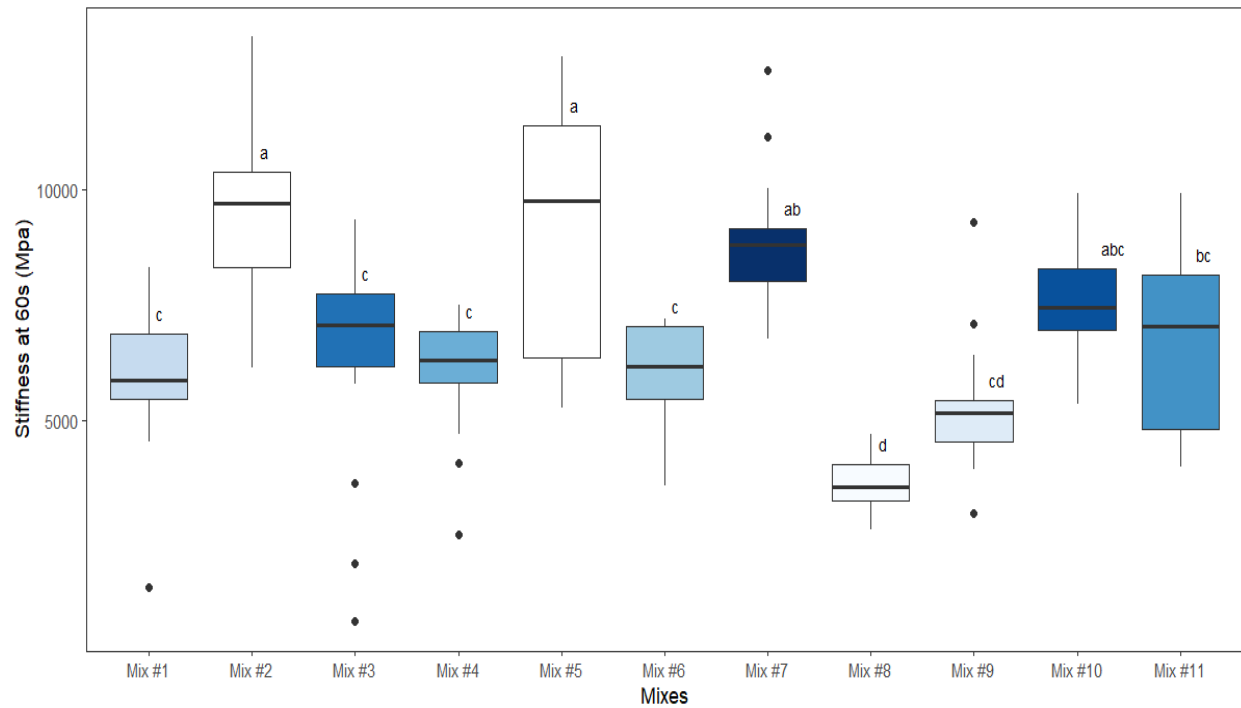


**Figure 8 – Compact Letter Display Boxplot for Creep Stiffness at -12 °C**

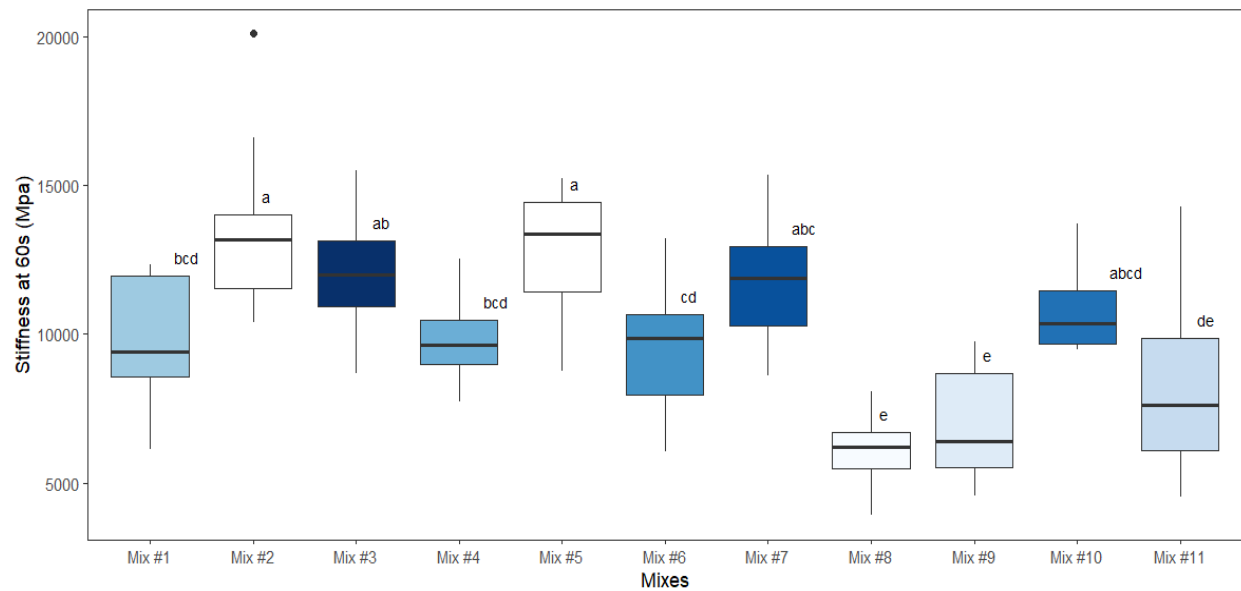


**Figure 9 – Compact Letter Display Boxplot for Creep Stiffness at -18 °C**

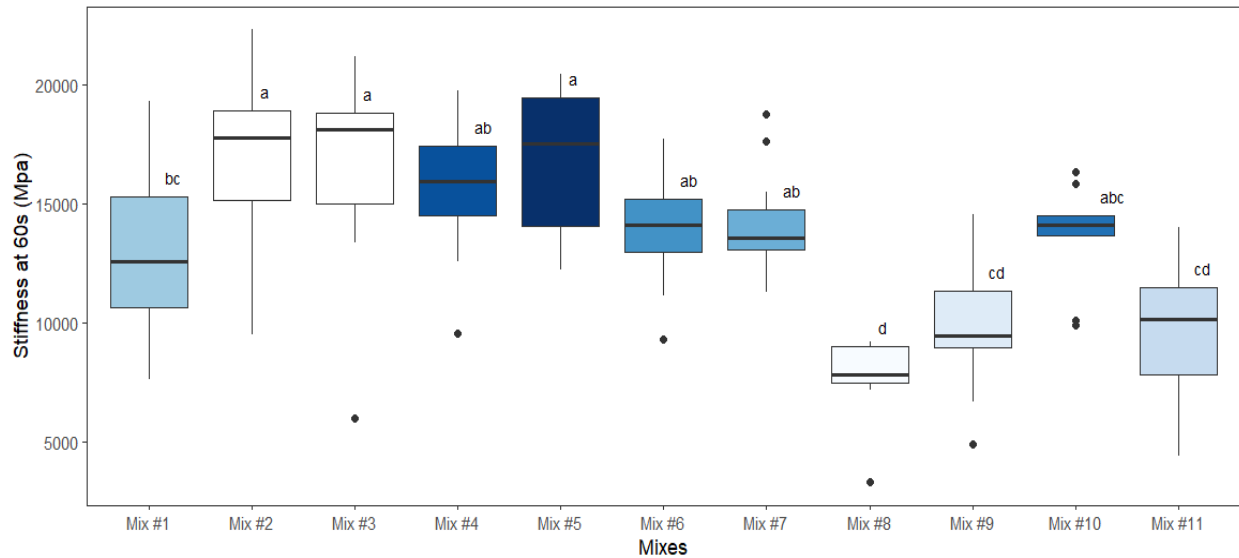


**Figure 10 – Compact Letter Display Boxplot for Creep Stiffness at -24 °C**

The results presented in Figure 6 through Figure 10 illustrate some interesting data; at relatively high temperatures (0 °C and -6 °C), there is enough variability in the results to allow for different groupings. Mixes #5, #7, and #10 belong in the high stiffness group; however, the high value is below 10,000 MPa, which is considered a limit for cracking potential. At a test temperature of -18 °C, all mixtures except #8, #9, and #11 belong to a group with creep stiffness values above the 10,000 MPa threshold. This means that none of the UDOT mixtures are expected to resist thermal cracking below a field temperature of -28 °C. Mixtures #8 and #9 (not UDOT mixtures) have the potential to resist cracking at a field temperature of -34 °C.

### 3.3 Semi-Circular Bending Illinois Flexibility Index Test (SCB-IFIT)

The semi-circular bending Illinois FI test is not favored by UDOT; however, it is one of the few tests that actually measure some form of fracture property. Based on this, it was included as part of this work for cases where there was enough material to perform the test.



### 3.3.1 Testing and Data Analysis

The summary of the average results, Standard Deviation, and coefficient of variation (COV) for fracture energy and Flexibility Index are shown in Table 4.

**Table 4 – FI and Fracture Energy for Eight Mixes.**

	<b>FI Index</b>	<b>Standard Deviation</b>	<b>COV</b>	<b>Fracture Energy (J/m<sup>2</sup>)</b>	<b>Standard Deviation</b>	<b>COV</b>
Mix #1	8.95	1.461	0.16	2178.3	114.29	0.05
Mix #2	7.60	2.740	0.36	2093.4	216.02	0.10
Mix #3	10.11	2.891	0.29	1931.4	151.95	0.08
Mix #4	12.35	3.802	0.31	2003.1	128.88	0.06
Mix #5	5.71	1.242	0.22	1855.6	157.63	0.08
Mix #6	10.76	0.658	0.06	1737.1	181.15	0.10
Mix #10	1.47	0.523	0.36	1445.9	150.40	0.10
Mix #11	2.42	0.290	0.12	1073.5	130.31	0.12

The result of Levene's test indicates that the variances of the Flexibility for different mix groups are not equal (heterogeneous). The p-value is 0.00239, less than 0.05; this means that the assumption of equal variances required for ANOVA and Tukey's test is unmet. The Games-Howell test, a different post hoc test with unequal variances, is used for the Flexibility Index. Figure 11 provides the Boxplot with a visual interpretation of the Games-Howell, where the Compact Letter Display (CLD) was used after the Games-Howell test to clarify the output of the confidence intervals where cells are grouped according to their means. Cells with the same color and letter belong to the same group.

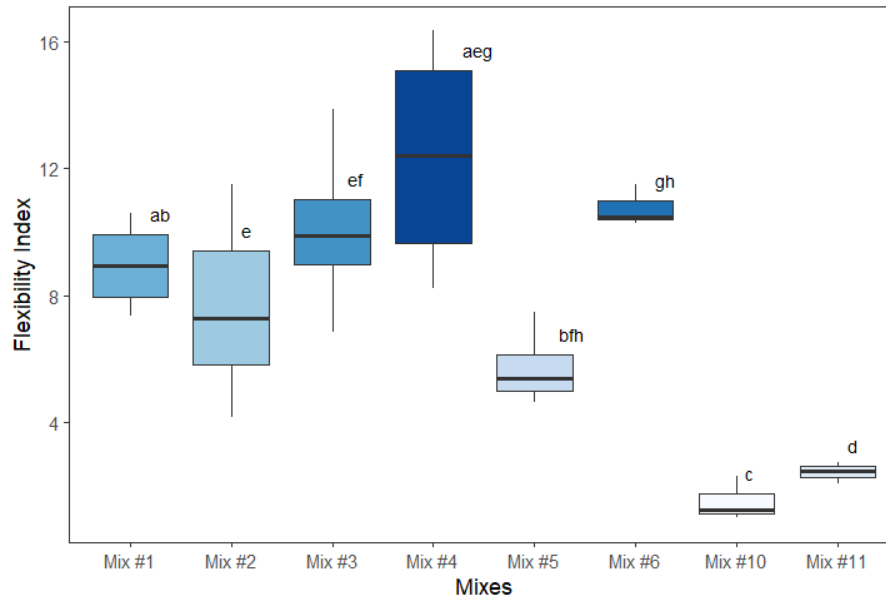


**Figure 11 - Compact Letter Display Boxplot for Flexibility Index and Visualization of Games-Howell Output.**

The results from Figure 11 show that Mixes #1 and #4 fall into the group with the highest FI values, while Mixes #10 and #11 fall into the group with the lowest FI values. However, when these groups are compared with those identified from the CT Index analysis, there is little overlap in terms of mixtures expected to perform well. Notably, Mixes #10 and #11 yield the lowest values in both tests. These findings are consistent with previous studies, which have concluded that although both the IDEAL-CT and the SCB-IFIT are intended to predict the same type of distress, they often show limited agreement.

As the Fracture Energy meets the assumption of equal variance, a Tukey's test was conducted to provide pairwise comparisons between the means of different mixes, followed by the Compact Letter Display (CLD) to clarify the ANOVA and Tukey tests' output. Figure 12 shows the CLD output Boxplot with the grouping of similar means.

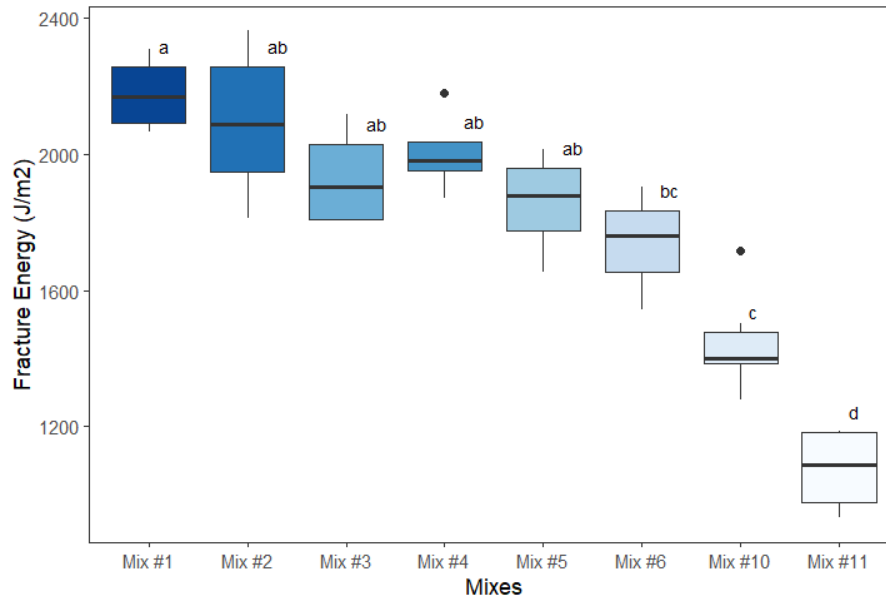


**Figure 12 - Compact Letter Display Boxplot for Fracture Energy and Visualization of Tukey-Test Output.**

A few observations were made based on the results. The highest fracture energy is observed for Mix #1 (UDOT Mix) and the lowest for Mix #11 (MnROAD Mix). This is consistent with previous results.

### 3.4 Comparison of Tests that Evaluate Cracking

Previous sections show the results for the IDEAL-CT, the BBR, and the SCB-IFIT tests. All of these tests were developed to evaluate the potential of asphalt mixtures for some form of cracking. IDEAL-CT and SCB-IFIT are performed at room temperature to evaluate intermediate-temperature cracking (i.e., fatigue-related cracking). The BBR is performed at low temperatures ( $<0^{\circ}\text{C}$ ) and is meant to evaluate low-temperature cracking. Table 5 shows how the grouping from the CLD evaluation compares in different tests. For those tests in which a high value is associated with mixtures likely to resist cracking, the mixtures in the 'a group' are shown together as 'likely to perform well'. Similarly, mixtures in the 'd group', representing the low values, are shown together.

**Table 5 - Comparison of Predictions from Tests Developed to Evaluate Cracking**

	Mixes likely to perform well based on groups	Mixes likely to perform poorly based on groups
<b>Test Parameter</b>		
<b><u>IDEAL-CT at 25 °C</u></b> High values are expected to resist fatigue cracking		
<b>CT Index</b>	1, 2, 6, 9	7, 10, 11
<b>Energy</b>	1, 5	8, 11
<b><u>SCB-IFIT at 25 °C</u></b> High values are expected to resist fatigue cracking		
<b>Flexibility Index</b>	1, 4	10, 11
<b>Energy</b>	1, 2, 3, 4, 5	11
<b><u>BBR Stiffness at 60 s</u></b> Low values are expected to resist thermal stress buildup		
<b>0 °C</b>	1, 6, 8, 9	5, 7, 10 <sup>‡</sup>
<b>-6 °C</b>	6, 8, 9	2, 5, 7, 10 <sup>‡</sup>
<b>-12 °C</b>	8, 9	2, 5, 7, 10
<b>-18 °C</b>	8, 9, 10	2, 3, 5, 7, 10
<b>-24 °C</b>	8, 9, 11*	2, 3, 4, 5, 6, 7, 10

\* Stiffness values are above the established threshold so thermal cracking would be expected, regardless of group, in all these mixes for environments with a low temperature reaching -34 °C.

‡ Stiffness values are below the established threshold, so thermal cracking would not be expected in environments with temperatures reaching -10 °C and -16 °C.

In general, Table 5 does not show good agreement between tests at intermediate temperatures when any index is used; only the energy shows some similarities between tests. Similar conclusions were obtained during previous work that compared both tests.

It should also be noted that mixture groups are different at low temperatures. This reinforces the need to adopt a low-temperature test for mixtures like the BBR since performance cannot be inferred from tests at intermediate temperatures.

### 3.4.1 Comparison to Published Data

Mixtures #10 and #11 were obtained from the MnROAD experiment. These same mixtures were tested at the University of Minnesota and the National Center for Asphalt

Technology, NCAT. This presents an opportunity to compare the results between different laboratories to ensure that results are repeatable. Table 6 shows a comparison of the intermediate-temperature tests, the CT Index, and the Flexibility Index.

**Table 6 – Comparison of Intermediate-Temperature Test Results**

	IDEAL-CT CT Index		Mean Difference	SCB-IFIT Flexibility Index	
	NCAT	U of U		NCAT	U of U
Mix ID					
<b>Mix #10 Cell 18</b>	52	42	21%	7.9	1.5
<b>Mix #11 Cell 21</b>	29	22	27%	9.5	2.4

The results shown in Table 6 indicate that the IDEAL-CT test will have the same ranking; however, the CT Index values can vary by as much as 27%. As Figure 2 shows, the coefficient of variation observed in this test can be as high as 25%. Thus, the observed difference is within the variability of the test. The values for the FI show a significantly large difference. As Table 4 shows, the FI has, in general, a high coefficient of variation of up to 36%. Fracture-type tests are notoriously variable.

Table 7 compares the results of the Bending Beam Rheometer at the University of Minnesota and the University of Utah. Table 7 shows encouraging results regarding the lab repeatability of the BBR test, with all values having a mean difference of less than 18% and only one value showing a mean difference greater than 12%.

**Table 7 – Comparison of Low-Temperature Test Results**

	Stiffness MPa			m-value	
	U of MN	U of U		U of MN	U of U
Mix #10			Mean		
Cell 18			Difference		
<b>0°C</b>	2831	3131	10%	0.31	0.33
<b>-12°C</b>	7039	7656	8%	0.17	0.17
<b>-24°C</b>	14028	13600	3%	0.07	0.08
Mix #11					
Cell 21					
<b>0°C</b>	2448	2197	11%	0.34	0.36
<b>-12°C</b>	5922	6673	12%	0.17	0.20
<b>-24°C</b>	12100	10083	18%	0.09	0.11

### 3.5 AMPT

The 11 mixtures were tested using the AMPT. The dynamic modulus and phase angle were determined at 4 °C, 20 °C, and 40 °C under four frequency conditions (0.01, 0.1, 1, and 10 Hz). Mixes #1 through #9 were tested at the Utah Department of Transportation Central Materials Lab as part of Phase II of this study. Mixes #10 and #11 were tested by Advanced Asphalt Technologies, LLC in Sterling, VA., during this phase.

Four samples were tested for mixtures 1 through 9; for mixtures 10 and 11, two samples were compacted, and each sample was tested twice. This resulted in 4 repetitions for each condition. The data collected for Mixtures #1 to #9 was discussed in the final report for Phase II of this study [4]. The data for Mixtures #10 and #11 is shown in Table 8 and Table 9, respectively.

**Table 8 – Dynamic Modulus Data for Mixture #10 (Cell 18)**

Temperature °C	Frequency Hz	Modulus ksi	CV %	Phase Angle	Std. Dev
<b>4</b>	10	2351.9	0.6	8.0	0.5
	1.0	1865.3	0.4	10.7	0.5
	0.1	1385.0	0.8	14.3	0.4
<b>20</b>	10	1104.2	1.8	17.9	0.7
	1.0	677.4	3.0	23.6	1.0
	0.1	368.0	5.2	28.7	1.4
<b>40</b>	10	272.0	5.2	31.2	0.6
	1.0	112.2	5.8	31.1	0.9
	0.1	47.3	4.2	26.1	1.8
	0.01	23.0	4.2	20.5	1.7

**Table 9 – Dynamic Modulus Data for Mixture #11 (Cell 21)**

Temperature °C	Frequency Hz	Modulus ksi	CV %	Phase Angle	Std. Dev
<b>4</b>	10	2493.7	13.1	7.6	0.4
	1.0	1941.1	19.0	10.5	0.5
	0.1	1394.4	25.6	14.5	0.7
<b>20</b>	10	1203.7	0.8	18.8	0.6
	1.0	704.4	2.8	25.7	1.1
	0.1	350.0	5.6	31.8	1.9
<b>40</b>	10	243.1	3.8	34.3	1.0
	1.0	87.8	6.0	33.3	1.7
	0.1	33.6	9.9	26.1	3.2
	0.01	24.3	9.6	20.7	3.2

The data was collected and dynamic modulus master curves were fitted to Equation 3 and Equation 4 using least squares minimization techniques. The resulting parameters that define the master curve are presented in Table 10.

**Table 10 – Master Curve Equation Parameters for the 11 Mixtures.**

<b>Dynamic Modulus Parameters</b>					
	Max E* <sup>‡</sup> , ksi	Min E*, Delta, ksi	Beta	Gamma	EA
Mix #1	3415.5	2.6	-1.02	-0.49	177905
Mix #2	3415.5	5.1	-0.923	-0.522	198743
Mix #3	3415.5	4.3	-0.975	-0.53	195105
Mix #4	3415.5	2.3	-0.833	-0.519	193450
Mix #5	3415.5	3.3	-0.999	-0.54	185238
Mix #6	3415.5	2.2	-1.029	-0.509	184000
Mix #7	3415.5	3.1	-1.332	-0.498	199399
Mix #8	3415.5	3.6	-0.493	-0.484	187284
Mix #9	3415.5	2.6	-0.675	-0.437	191521
Mix #10	3415.5	9.3	-1.052	-0.622	214926
Mix #11	3415.5	3.3	-1.225	-0.489	216622

<sup>‡</sup>The value of Max E\* was fixed for all mixtures based on Hirsch Model.



## Chapter 4.0 Model Development

### 4.1 Overview

In this chapter, the data collected from nine different asphalt mixtures is analyzed along with two new mixes to determine the relation between IDEAL-CT and the dynamic modulus parameters. Data from the Bending Beam Rheometer is added to the model, and then the different models that predict the dynamic modulus master curve are used to predict pavement performance using AASHTOWare Pavement ME® software.

During Phase II of this project, relations were developed that predict the beta and gamma parameters of Equation 3 using IDEAL-CT data. These predictive equations are:

$$\text{Beta} = 4 \times 10^{-8} (\text{Energy})^2 - 7 \times 10^{-4} (\text{Energy}) + 1.9939 \quad \text{Equation 6}$$

$$\text{Gamma} = 1.1 \times 10^{-3} (\text{CT Index}) - 0.5964 \quad \text{Equation 7}$$

Where 'Energy' is the fracture energy in J/m<sup>2</sup> and CT Index is the cracking tolerance index, both obtained from the IDEAL-CT test. Equation 6 resulted in an R-square of 0.83, while Equation 7 had an R-square of 0.67. While the prediction of the dynamic modulus is far from perfect, with a difference of about 20%, it allowed us to develop the curve with a significantly reduced effort (i.e., hours vs. weeks), thus balancing rigor with practicality.

For this phase, the relationship in Equation 6 and Equation 7 were verified using Mixtures #10 and #11. Following the verification, the low-temperature mixture properties obtained from the BBR were incorporated into the predictive equations.

Finally, based on the analysis, relations were developed to predict the dynamic modulus master curve based on IDEAL-CT tests. Comparisons between measured values and predicted values will be shown.

## 4.2 Verification of Predictive Relation

Using Equation 6 and Equation 7, the values of the parameters beta and gamma were predicted and compared to the fitted values shown in Table 10. The results are shown in Table 11.

**Table 11 - Prediction of Beta and Gamma Parameters for Mixes #10 and #11**

		Mix #10	Mix #11
<b>CT Index</b>		42	26
<b>Energy, J/m<sup>2</sup></b>		7180	4923
<b>Beta</b>	Fitted <sup>‡</sup>	-1.052	-1.225
	Predicted	-0.970	-0.483
	Error from Fitted, %	7.8	60.6
<b>Gamma</b>	Fitted <sup>‡</sup>	-0.622	-0.489
	Predicted	-0.550	-0.568
	Error from Fitted, %	11.5	-16.1

<sup>‡</sup> Fitted refers to values obtained using Master Solver routine.

Table 11 shows that the model is able to predict the values for Mix #10 with reasonable accuracy. The difference in fitted and predictive values is less than 8% for the Beta parameter and less than 12% for the Gamma parameter. For Mix #11, the error is significant, with a difference of 60% for the Beta parameters. This lack of prediction accuracy was expected, given that Mix #11 was formulated with a PG 58-34 asphalt binder. It was documented in Phase II that the relation was developed for mixtures formulated with PG 64-XX binders; Mixture #7 (PG 58-28) was excluded from Equation 6 and Equation 7 developments. It can be stated that Mixes #7 and #11 belong to a different family of mixtures.

Figure 13 shows a plot of the Beta parameter as a function of fracture energy. It is clear that Mix #10, which is a MnROAD PG 64-34 mix, follows the pattern predicted by Equation 6. Mixes #7 and #11, formulated with a PG 58-XX asphalt binder, do not follow the equation. Figure 13 also shows that mixtures made with the softer binder

follow the same form of Equation 6 but with an offset. However, given that only two mixtures were available for testing, the relation cannot be verified. Testing of mixtures from different families would be required to validate this statement. It should be noted that the PG 64-XX is the standard binder used in surface mixtures throughout the state of Utah.

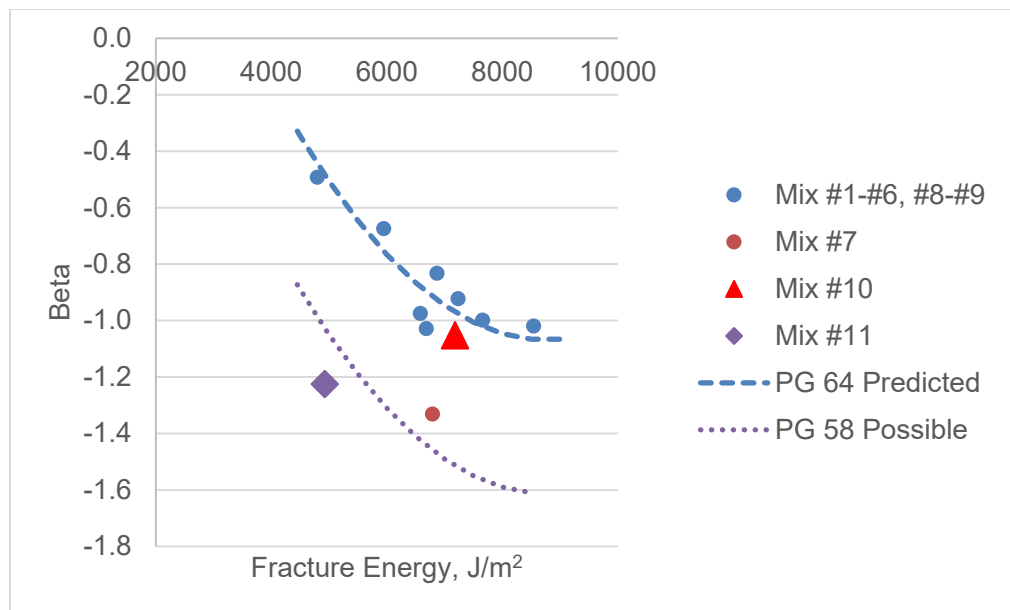


**Figure 13 – Relation Between Fracture Energy and Beta Parameter**

Figure 14 shows the relation between the Gamma parameter and the CT Index. Equation 7, which predicts the Gamma parameter, is not as good a predictor as Equation 6. Nonetheless, the mixes made with PG 58-XX are grouped together. Mix #10 does not fall close to the prediction line.

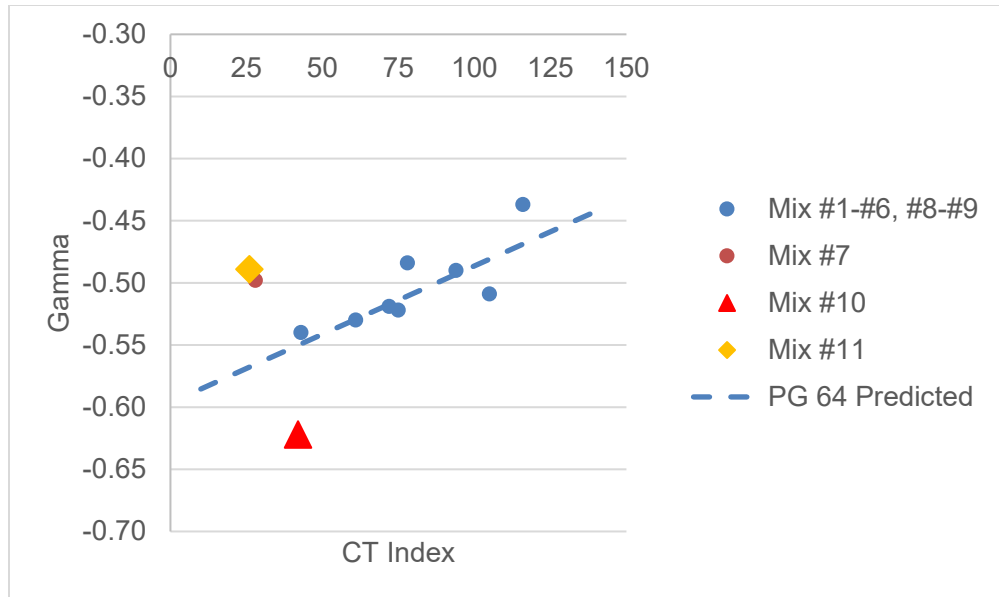


**Figure 14 – Relation Between CT Index and Gamma Parameter**

### 4.3 Incorporation of Low-Temperature Data

Developing equipment that records the dynamic modulus of asphalt concrete at very low temperature or high frequencies has proven to be mechanically challenging and unrealistic because of the high stiffness values of the asphalt mixture. Hence, researchers and engineers have relied on predictive models that estimate the low-temperature modulus and assumed functional forms to overcome this limitation.

Task 3 of the project addresses the limitations of existing predictive models for estimating maximum dynamic modulus ( $E_{max}^*$ ) at low temperatures, by incorporating low-temperature values derived from Bending Beam Rheometer (BBR) tests into the master curve formulation. Unlike prior approaches that fixed the maximum dynamic modulus  $E_{max}^*$  at 3,415.5 ksi, a default value in the Master Solver derived from the Hirsch model, this study directly extrapolates measured BBR data to verify if it better reflects the asphalt mixture's behavior under high-frequency or low-temperature loading conditions.

The 11 asphalt mixtures used in this research were evaluated using the BBR in accordance with AASHTO TP 125-16. The BBR test on asphalt mixtures can be

performed with minimal material. Flexural creep stiffness measurements at -24°C were collected and extrapolated to a loading time of 0.01 seconds, corresponding to a frequency of approximately 100 Hz. This timeframe was assumed to represent the typical influence duration of vehicular loading at high frequencies and aligns with the glassy region of asphalt behavior. The extrapolated stiffness values at 0.01 seconds were used as the  $E_{max}^*$  value, representing the upper bound or upper asymptote of the dynamic modulus master curve.

#### 4.3.1 Hirsch Model

Work by Christensen and Bonaquist [14], [15] proposed the use of a Hirsch Model, based on volumetric properties to predict the upper asymptote, or  $E_{max}^*$  of the dynamic modulus master curve.

The volumetric properties of the asphalt sample consist of the fraction of aggregate voids filled with asphalt (VFA) and the void in the mineral aggregate (VMA). This is the basic building block for generating the Hirsch model. The Hirsch model, being the generally accepted and available predictive model, is used in the MEPGD guide, and uses Equations 8 through 10 to determine the maximum dynamic modulus.

$$E_{max}^* = P_c \left( 4,200,000 \left( 1 - \frac{VMA}{100} \right) + 3G \left( \frac{VFA \cdot VMA}{10,000} \right) \right) + \frac{1 - P_c}{\left( \frac{1 - \frac{VMA}{100}}{4,200,000} + \frac{VMA}{3G^x(VFA)} \right)}. \quad \text{Equation 8}$$

Equation 8 assumes that the Poisson's ratio for asphalt materials is 0.5, indicating an incompressible material where  $G$  is the limiting shear binder modulus (Equation 9) and  $P_c$  is the contact factor (Equation 10). However, this assumption remains a considerable debate to this day, as several studies have shown that asphalt mixtures can exhibit Poisson's ratios ranging from 0.3 to 0.45 under certain temperatures and loading conditions. This variation occurs because asphalt's viscoelastic behavior changes with temperature and loading rate, making it unlikely that a single, fixed value can accurately represent all conditions. Such assumptions in predictive models can lead to inaccuracies, particularly in calculating shear and elastic moduli, ultimately affecting the reliability of pavement performance predictions. The

limiting shear modulus  $G$  of the binder is equivalent to the effective binder modulus ( $E_b^1$ ) from Equation 9.

$$E_b^1 = \frac{t_f E_b E_g}{(t_f - t_T) E_g + t_T E_b} \quad \text{Equation 9}$$

Where  $t_f$  is the binder film thickness,  $E_g$  is the glassy modulus assumed as 1 GPa (1,450,000 psi),  $E_b$  is the binder modulus, and  $t_T$  is the transition zone between the aggregate and binder. The value of the contact factor  $P_c$  is obtained using Equation 10, which is dependent on the VMA and VFA of asphalt.

$$P_c = \frac{\left(20 + \frac{435,000(VFA)}{VMA}\right)^{0.58}}{650 + \left(\frac{435,000(VFA)}{VMA}\right)^{0.58}} \quad \text{Equation 10}$$

#### 4.3.2 Comparison of Results

Compared to the default Hirsch model value of 3,415.5 ksi, the  $E_{max}^*$  values obtained from the BBR revealed significant variation across mixtures. For example, Mix #3 exhibited an  $E_{max}^*$  approximately 32% higher than the Hirsch-predicted value, while Mix #6 had a value about 37% lower. This shows that although samples may belong to the same group or within the same PG range, applying a universal constant for all mixtures, especially in climates susceptible to thermal cracking, can cause overpredictions or underpredictions in the master curve model. It also shows that the volumetric properties of asphalt concrete have limited influence on its modulus since the mastic is expected to dominate the behavior at this temperature. Therefore, using a Hirsch model, which has a foundational building block on volumetric properties to predict the asymptote of the maximum  $E_{max}^*$ , does not fully represent asphalt mixture properties. Table 12 presents BBR-derived versus Hirsch-predicted  $E_{max}^*$  values, highlighting the discrepancies and the need for measured inputs.

**Table 12 – Maximum Dynamic Modulus for Predicted and Measured Values**

Lab ID	VMA	VFA	Max E*, ksi (Hirsch Model)	Max E*, ksi (BBR-derived data)
Mix #1	14	75	3415.5	3027.8
Mix #2	14	75	3415.5	3430.6
Mix #3	14	75	3415.5	4522.5
Mix #4	14	75	3415.5	4190.3
Mix #5	14	75	3415.5	4002.6
Mix #6	14	75	3415.5	2136.3
Mix #7	14	75	3415.5	2507.6
Mix #8	14	75	3415.5	1870.0
Mix #9	14	75	3415.5	2151.8
Mix #10	14.6	73.5	3415.5	3567.7
Mix #11	14.6	73.5	3415.5	2558.1

To evaluate the influence of these measured values on master curve generation, a sigmoidal model was fitted using the BBR-derived  $E_{max}^*$  as the upper asymptote. Figure 15 shows the resulting master curves compared against those constructed using the Hirsch model for Mix #1; all other mixes are shown in Appendix A. The curves based on BBR-derived  $E_{max}^*$  are assumed to offer a more realistic representation of asphalt stiffness under low-temperature and high-frequency loading conditions, capturing mix-specific variations in binder and aggregate interaction.

The updated master curves were further integrated into AASHTOWare Pavement ME® software as Level 1 inputs. Performance predictions based on these measured values should indicate better alignment with observed cracking trends in field data, particularly for bottom-up fatigue cracking. More on this issue is discussed in the next section. This integration represents a step forward in moving from empirical estimations to mechanistically validated, mixture-specific modulus inputs, thereby improving the accuracy of pavement life predictions and optimizing material usage.

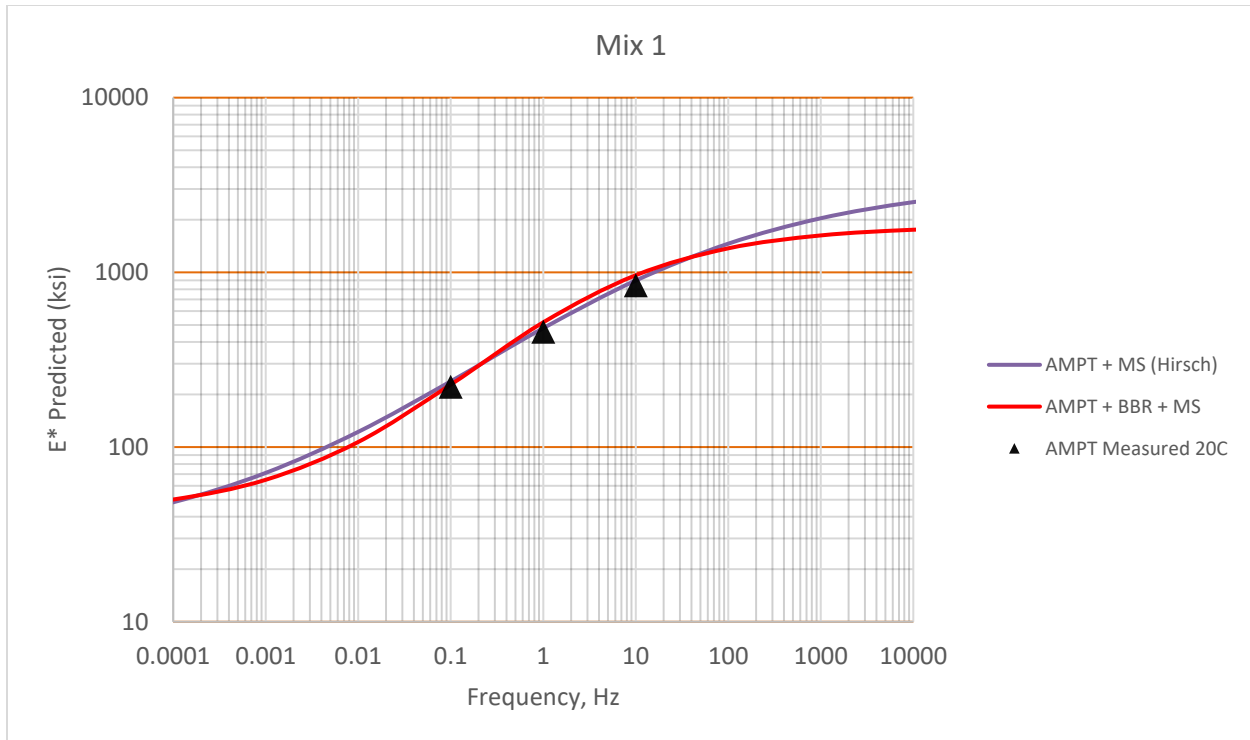


**Figure 15 – Comparison of Different Model Predictions for Mix #1**

#### 4.4 AASHTOWare Verification

To assess the reliability of using measured low-temperature dynamic modulus values in mechanistic-empirical pavement design, AASHTOWare Pavement ME® was used to predict the performance of a pavement.

The pavement structure modeled in AASHTOWare consists of a 13-inch asphalt mix surface layer (Mixes #1 through #11), underlain by 12 inches of base and 14 inches of sub-base over an A-6 subgrade. The asphalt mix for all simulations had an effective binder content of 11.0% and air voids of 6.5% at construction. The design considers an initial average daily truck volume of 9,000 in 2024, with a projected cumulative total of approximately 11 million trucks over the next 10 years.

Dynamic modulus master curves were constructed for each of the 11 asphalt mixtures using different combinations of data inputs. The resulting dynamic modulus data was used as input into the AASHTOWare Pavement ME® design software to



evaluate how they influence predicted pavement performance outcomes, particularly regarding fatigue cracking and rutting. It should be noted that the  $E^*$  data is not part of the thermal cracking model as it only represents intermediate-temperature properties.

Four different modeling approaches were adopted to obtain dynamic modulus data and implemented in AASHTOWare:

**Model 1:** Hirsch Model + AMPT Data + Master Solver (AMPT + MS)

This approach used the Hirsch model to predict maximum dynamic modulus ( $E_{max}^*$ ), combined with dynamic modulus data obtained from AMPT testing at intermediate and high temperatures. A master curve was constructed using the Master Solver fitting tool, following NCHRP Report 9-29 guidelines. This served as a baseline model reflecting current standard predictive practices.

**Model 2:** Measured BBR Data + AMPT Data + Master Solver (BBR + AMPT)

In this model,  $E_{max}^*$  values were derived from low-temperature BBR measurements, extrapolated to 0.01 seconds to reflect low-temperature and high-frequency loading (approximating the glassy state of asphalt) conditions. These values were integrated with AMPT data from intermediate and high temperatures to construct the master curve. This approach reflects a higher-level input consistent with Level 1 in the MEPDG hierarchy.

**Model 3:** Hirsch Model + IDEAL-CT Parameters (IDEAL-CT + Fixed E)

The  $E_{max}^*$  from the Hirsch model was retained, but sigmoidal curve fitting parameters ( $\alpha$ ,  $\beta$ ,  $\gamma$ ) were extracted from IDEAL-CT results performed at intermediate temperatures. This hybrid model incorporated laboratory-derived fracture parameters into an otherwise predictive framework.

**Model 4:** Modeling Measured Inputs (BBR + IDEAL-CT)

This model represents the highest implementation of this research, using  $E_{max}^*$  values obtained from BBR testing and sigmoidal fitting parameters ( $\alpha$ ,  $\beta$ ,  $\gamma$ ) obtained from IDEAL-CT results. This model provides a fully data-driven representation of the dynamic modulus master curve across the frequency-temperature domain.

Each model was implemented across all 11 mixtures, with dynamic modulus values calculated for a matrix of five temperatures (14°F to 130°F) and six loading frequencies (0.1 to 25 Hz). The master curves generated were input into AASHTOWare and used to simulate 10-year pavement performance under standard traffic and environmental conditions. The simulation outputs revealed key distinctions among the models.

#### 4.4.1 Fatigue Cracking

Figure 16 shows that there are some predicted variations in bottom-up fatigue cracking across the different mixtures. Model 4 (BBR + IDEAL-CT) did show some differences in Mixes #6, #7, #8, and #11. However, the predicted fatigue cracking ranges between 0.5 and 1.5% for mixes evaluated; this is a negligible difference in terms of fatigue cracking performance. The results indicate that the simplest model (Model 3) results in the same relative performance predictions as the more involved model (Model 2) or the current practice (Model 1). While adding the data obtained from the BBR (Model 4) resulted in notable differences in some mixtures, **the performance predictions would not likely result in changes to the design.**

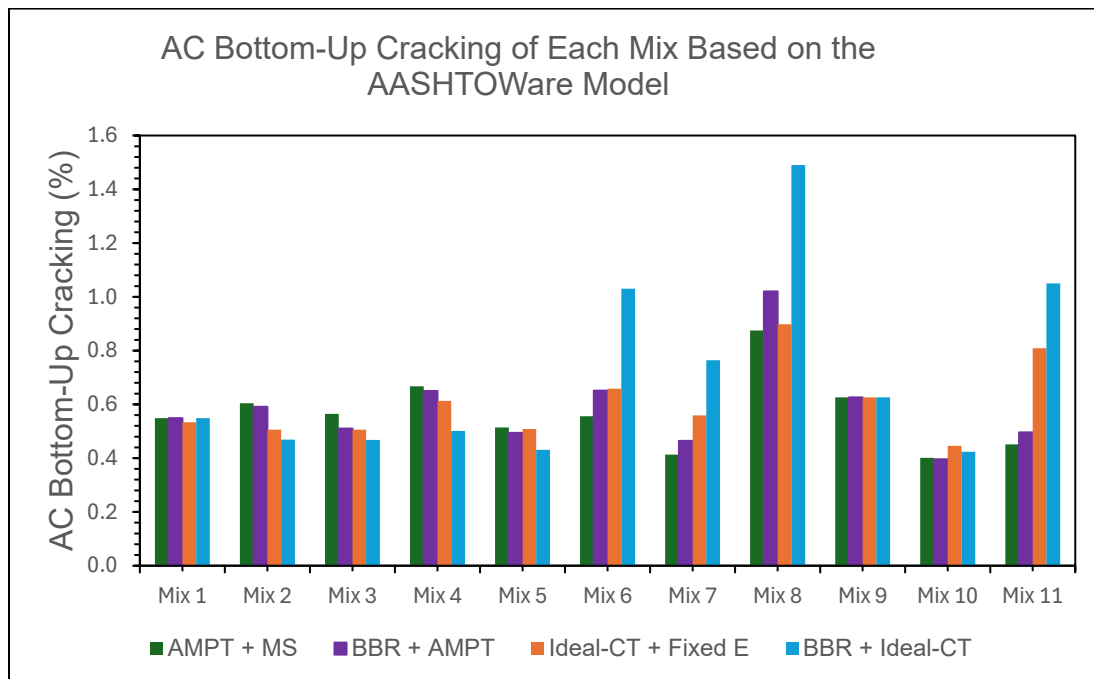


**Figure 16 – AC Bottom-Up Cracking of Each Mixture Across the Models**

#### 4.4.2 Rutting

Figure 17 shows the different performance predictions for rutting. Differences among models were minimal in rutting predictions as all the values were below 0.03 inches. Model 4 did show some variations across various mixes; it is not known if these differences would be amplified in mixtures susceptible to rutting.

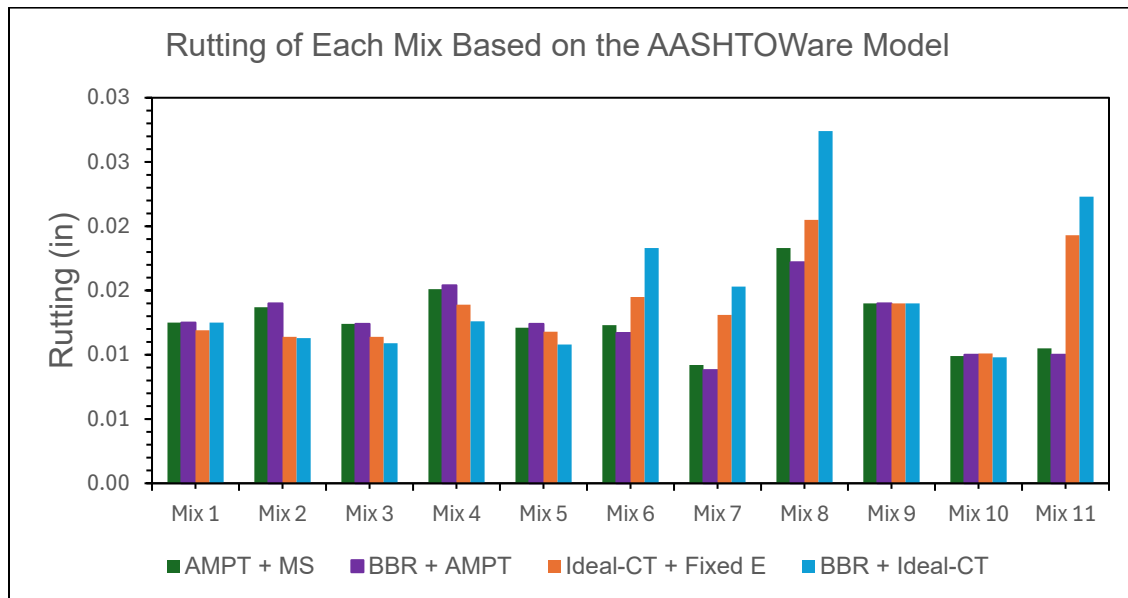


**Figure 17 – Rutting of Each Mixture Across the Models**

The results obtained from having different inputs in the AASHTOWare Pavement ME® software indicate that for most mixtures, the difference in performance predictions when the dynamic modulus master curve is obtained through alternate methods would not result in a different pavement design. This is encouraging as it supports the use of a simpler methodology.

In some mixtures, the development of the dynamic modulus master curve using BBR-measured data instead of the Hirsch relations results in different limiting values, but, given that dynamic modulus is not an input to the thermal cracking model, the predictions are not different enough that they would affect the design. Nonetheless, it should be noted that the data obtained from the BBR could be used as input to the thermal cracking model in AASHTOWare Pavement ME®.

## 4.5 Review

Two new asphalt mixtures from the MnROAD Research Program (Cells 18 and 21) were used to validate the relationships developed using nine previously studied mixtures. The results confirmed the validity of these relationships for a specific group of mixtures made with PG 64-XX binders. It is hypothesized that similar relationships may exist for mixtures using different binder grades; however, only two such mixtures were available for analysis, which is insufficient to validate this hypothesis at this time.

Measured low-temperature data obtained using the Bending Beam Rheometer (BBR) were incorporated into the dynamic modulus master curve. The results suggest that predicting the limiting dynamic modulus ( $E^*_{\max}$ ) using only volumetric relationships may overlook important interactions between the mixture components. The BBR measurements indicate that these interactions can be significant, likely resulting in differences in performance. Models that incorporate measured low-temperature  $E^*_{\max}$  values (specifically Models 2 and 4) offer additional insight into asphalt mixture behavior at high frequencies and low temperatures; this information is not captured by conventional methods. Generalized models, like the Hirsch model, may misrepresent the behavior of site-specific materials. However, it is important to clarify that dynamic modulus is not the primary input for predicting low-temperature cracking. As a result, the overall impact of this approach on pavement performance predictions remains limited.

Finally, the various methods used to develop the dynamic modulus of asphalt mixtures were evaluated on a standard pavement using performance predictions generated by the AASHTOWare Pavement ME® design software. The results showed that the differences in predicted pavement performance would not result in a different pavement design, regardless of the method used to obtain the dynamic modulus. This indicates that using IDEAL-CT data to estimate the input parameters for the dynamic modulus master curve will not affect pavement design outcomes. While direct measurements of dynamic modulus at different temperatures and frequencies might still be desired under some circumstances, the time and effort required to obtain such

measurements are not justified when the same conclusions could be reached using alternate, single-value parameters from tests used during the mix design method.

It should be clear, however, that the models developed are based on specific asphalt mixtures prepared using PG 64-XX binders. More data is required to extend the models to other types of mixtures.

# **Chapter 5.0 Summary and Conclusions**

## **5.1 Summary**

This research focused on expanding and refining the methodology for predicting the dynamic modulus master curve using single-parameter asphalt mixture tests. Specifically, the relations developed in earlier phases were broadened to include additional asphalt mixtures, including two obtained from MnROAD, greatly enhancing the applicability of the predictive model. Low-temperature properties for all 11 mixtures (nine from Phase II and two new ones) were incorporated into the dynamic modulus master curve, enabling the integration of BBR test results into pavement design and replacing reliance on the Hirsch model. The research produced complete master curves and quantified prediction errors by comparing measured and predicted values, validating and refining the equations developed using AASHTOWare Pavement ME® results.

## **5.2 Mixture Testing**

Testing of 11 asphalt mixtures using the IDEAL-CT revealed a wide range of performance characteristics, with CT Index values varying from just over 20 to nearly 120, and fracture energy ranging from less than 5 kJ/m<sup>2</sup> to a high of 9 kJ/m<sup>2</sup>. Notably, Mixtures #1 through #6, though designed for the same environmental conditions, using identical specifications and binder grades, exhibited differences in performance. These findings highlight the inherent variability among asphalt mixtures and reinforce the importance of performance-based testing to ensure that materials meet design expectations under real-world conditions.

The results from low-temperature testing reveal notable trends in mixture behavior at various low temperatures. At relatively high test temperatures (0 °C and -6 °C), sufficient variability was observed to allow classification into different stiffness groups, with Mixtures #5, #7, and #10 in the high-stiffness category, though still below

the 10,000 MPa threshold commonly associated with increased cracking risk. At -18 °C, all mixtures except #8, #9, and #11 exhibited creep stiffness values exceeding 10,000 MPa, indicating limited resistance to thermal cracking in field temperatures below -28 °C. Only Mixtures #8 and #9 demonstrated the potential to resist thermal cracking down to a field temperature of -34 °C, suggesting that most UDOT mixtures may require modification to perform adequately under extreme cold conditions.

### 5.3 Model Development and Validation

This study incorporated measured low-temperature data from the Bending Beam Rheometer (BBR) into the development of dynamic modulus master curves. The findings indicate that relying solely on volumetric relationships to predict the limiting dynamic modulus ( $E^*_{max}$ ) may fail to capture key interactions among mixture components, which can significantly influence performance. Models that include measured low-temperature  $E^*_{max}$  values, particularly Models 2 and 4, provide a greater understanding of asphalt mixture behavior that is not reflected in the Hirsch model. However, since dynamic modulus is not the primary parameter used in predicting low-temperature cracking, the direct impact of this enhanced modeling approach on pavement performance predictions remained limited.

The results from using different input methods in AASHTOWare Pavement ME® indicate that, for most mixtures, performance predictions remain largely unaffected by the method used to generate the dynamic modulus master curve. This finding is encouraging, as it validates the use of simplified approaches for estimating the dynamic modulus master curve without compromising the accuracy of pavement performance predictions.

### 5.4 Conclusions

This research series has established a foundation for developing a practical relationship between material tests currently employed by UDOT; namely, the Bending Beam Rheometer (BBR) for low-temperature behavior and the IDEAL-CT test for

intermediate-temperature cracking resistance, and the dynamic modulus ( $E^*$ ) master curve values required as Level 1 inputs in AASHTOWare Pavement ME® design software. The proposed approach aims to streamline the testing process by enabling the selection of a representative  $E^*$  master curve directly tied to the asphalt mixture used, without the need for time-consuming dynamic modulus testing. While direct measurements of the  $E^*$  and the corresponding master curve remain valuable, the developed correlations offer a reliable approximation that significantly reduces testing effort and time. This capability presents several key benefits:

- (1) a direct linkage between material properties and pavement design, enabling more accurate life-cycle cost analyses;
- (2) the use of project-specific material data rather than generalized national averages; and
- (3) a substantial reduction in testing duration, from weeks to days, thus enhancing efficiency in pavement design and evaluation.

Ultimately, this research established a practical and streamlined process for generating dynamic modulus master curves suitable for direct input into AASHTOWare Pavement ME®, further simplifying testing procedures while enhancing the accuracy and material selection during pavement designs.

## **5.5 Limitations and Challenges**

Availability of different mixtures was identified as a limitation of this study. The models developed were validated for typical surface mixtures, prepared with PG 64-XX asphalt binder. Further testing should be done to develop relations for mixtures made with different binder grades.

The high-temperature region of the dynamic modulus master curve was not investigated during this work and needs to be incorporated for completeness.



# **Chapter 6.0 Recommendations and Implementation**

## **6.1 Recommendations**

It is recommended that the relations and procedures developed as part of this research be incorporated into the pavement design methodology. While it is recognized that there is benefit in testing the dynamic modulus of asphalt mixtures, the time and effort required for such testing limit its application to only specialty mixtures. For typical surface mixtures used by UDOT, the relations developed provide adequate inputs for pavement design.

It is recommended that further research be conducted to incorporate the high-temperature properties of the mix into the dynamic modulus master curve. This information can be obtained from tests such as the Hamburg Wheel Tracking Device currently used by UDOT.

It is recommended that further research be conducted to develop a cost analysis of different asphalt mixtures as a function of pavement performance. This will help develop better life-cycle analysis models.

## **6.2 Implementation Plan**

The work presented in this report presents a unique opportunity to obtain the input parameters needed for Level 1 performance predictions in AASHTOWare Pavement ME®. This can be implemented immediately thanks to an accompanying spreadsheet provided.

A key outcome of this work is the ability to directly link pavement design with asphalt mix design and even construction quality control. It is envisioned that eventually the process will incorporate the following six steps.

Step 1: Mixture Selection – It has been established that the CT Index of a mixture can relate to potential performance; therefore, asphalt mixtures can be separated into three categories based on their CT Index:

- Premium: CT Index  $\geq 100$
- Regular:  $60 \leq \text{CT Index} \leq 99$
- Economy: CT Index  $\leq 59$

While these values are used as an example, Figure 2 shows that these are realistic numbers.

Step 2: Mixture Cost – It is reasonable to assume that Premium mixtures will have a higher cost when compared to Regular or Economy. This reflects not only the higher quality of materials and the added requirements for mix designs, but also tighter quality control processes. The specific cost of each type of mix can be quantified or determined through other methods.

Step 3: Pavement Design – A pavement section can be designed using AASHTOWare Pavement ME®. The relations developed as part of this work allow Premium, Regular, and Economy mixes to be assigned different dynamic moduli as Level 1 design inputs. Depending on factors such as traffic and climate, the resulting pavement performance could vary (e.g., 20 years for Premium, 15 years for Regular, 10 years for Economy), though in some cases the models may show no significant difference between mixes.

Step 4: Life Cycle Cost Analysis (LCCA) – Both mix cost and performance-related costs (e.g., maintenance, shorter service life) can be quantified. Designs can then be optimized based on life-cycle cost or other project priorities. The result is the selection of the most cost-effective mixture for the pavement design.

Step 5: Mixture Design – Once a mixture type is selected, the design must meet the CT Index requirement for that category. For instance, a Premium mix must achieve a CT Index  $\geq 100$ , while a Regular mix must exceed 61. Because the IDEAL-CT test is simple and widely available, setting such requirements is practical.

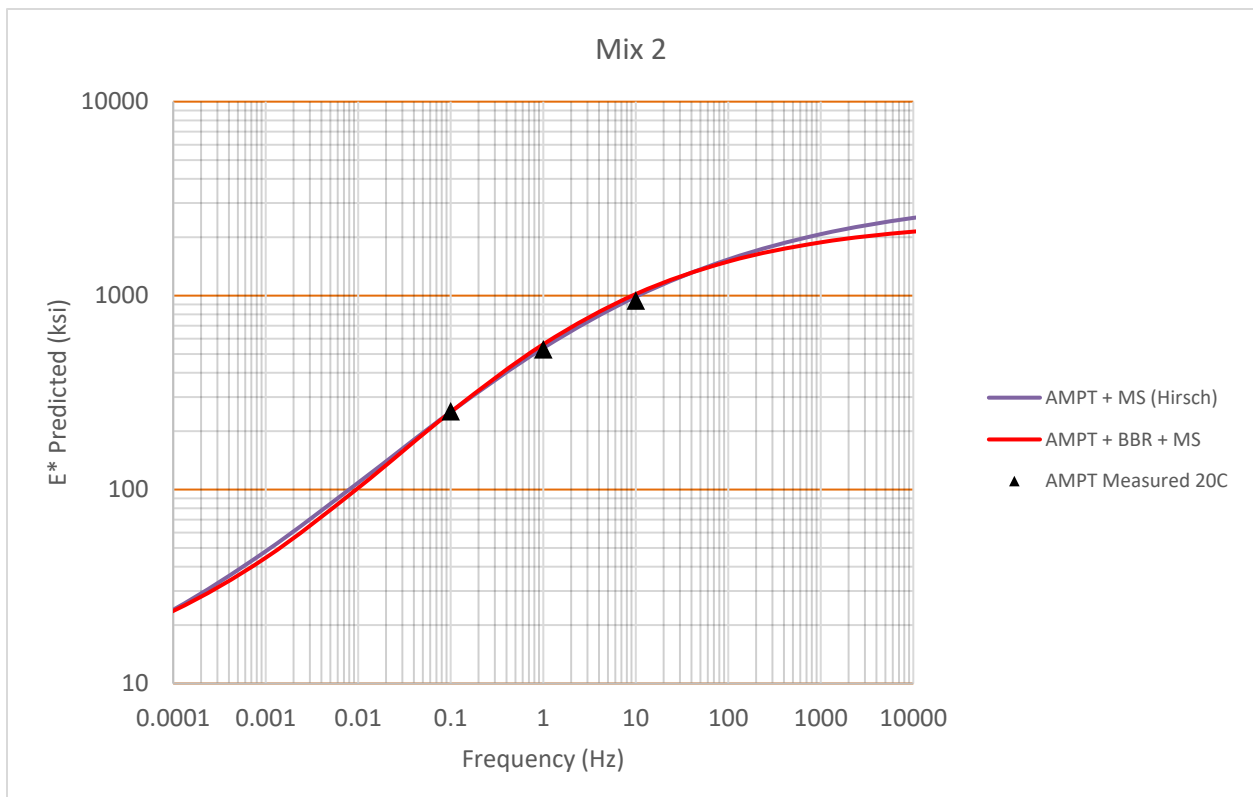
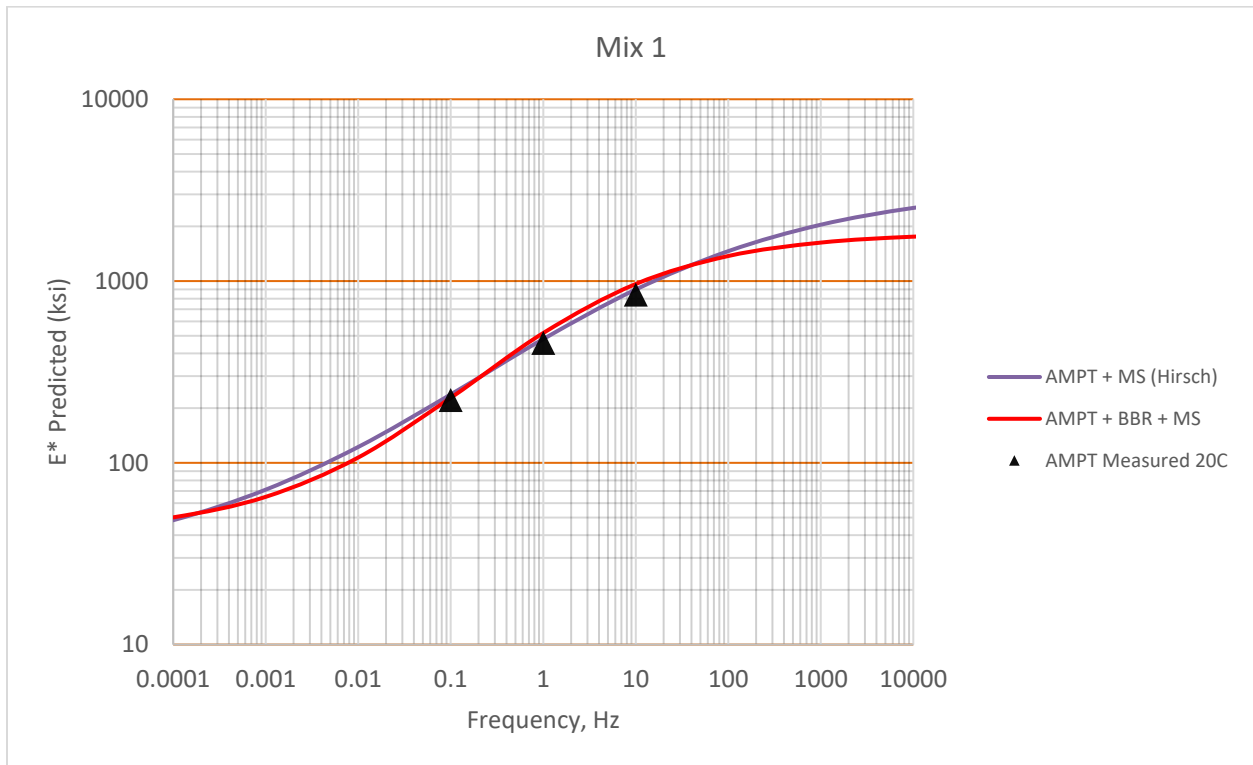
Step 6: Pavement Construction – During construction, asphalt mixtures are sampled, prepared, and tested with the IDEAL-CT to confirm they meet the specified CT Index. If results fall outside the required range, penalties can be applied. Again, the ease of the IDEAL-CT test makes this step feasible.

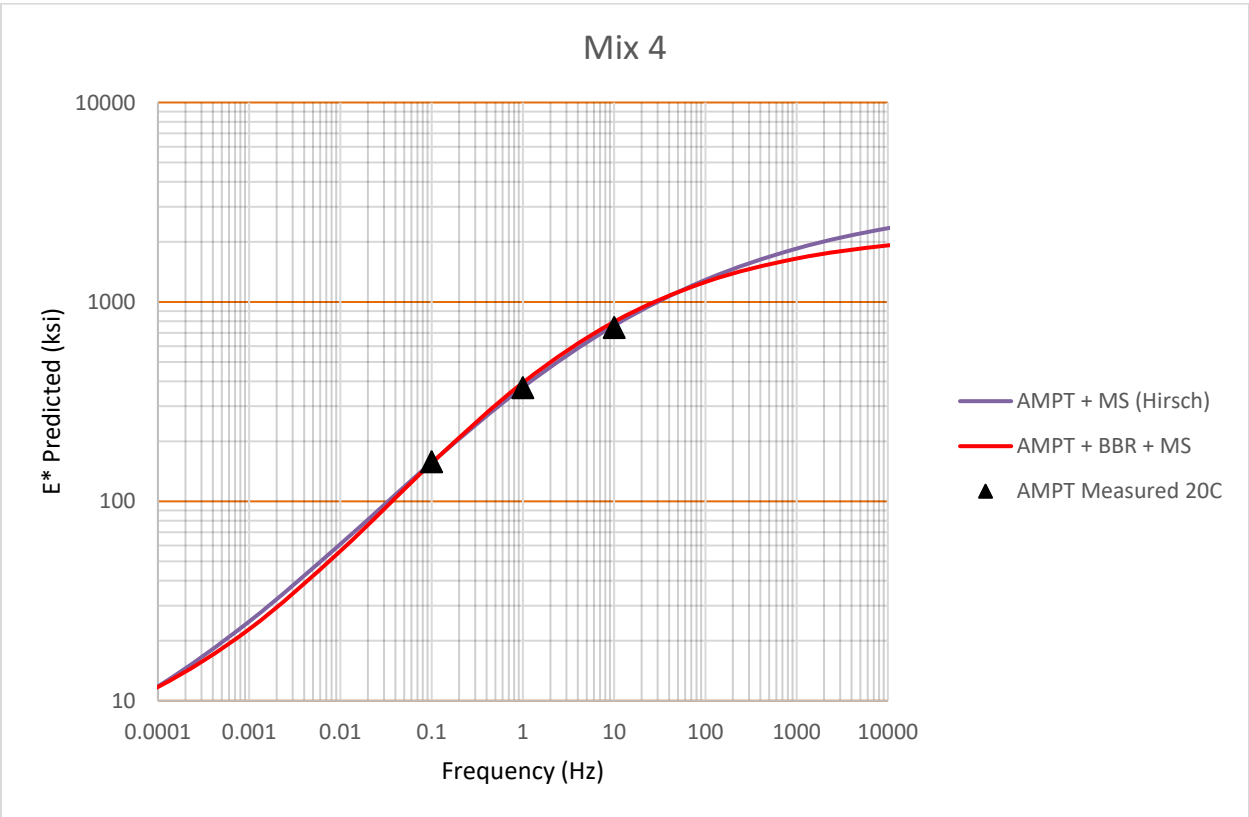
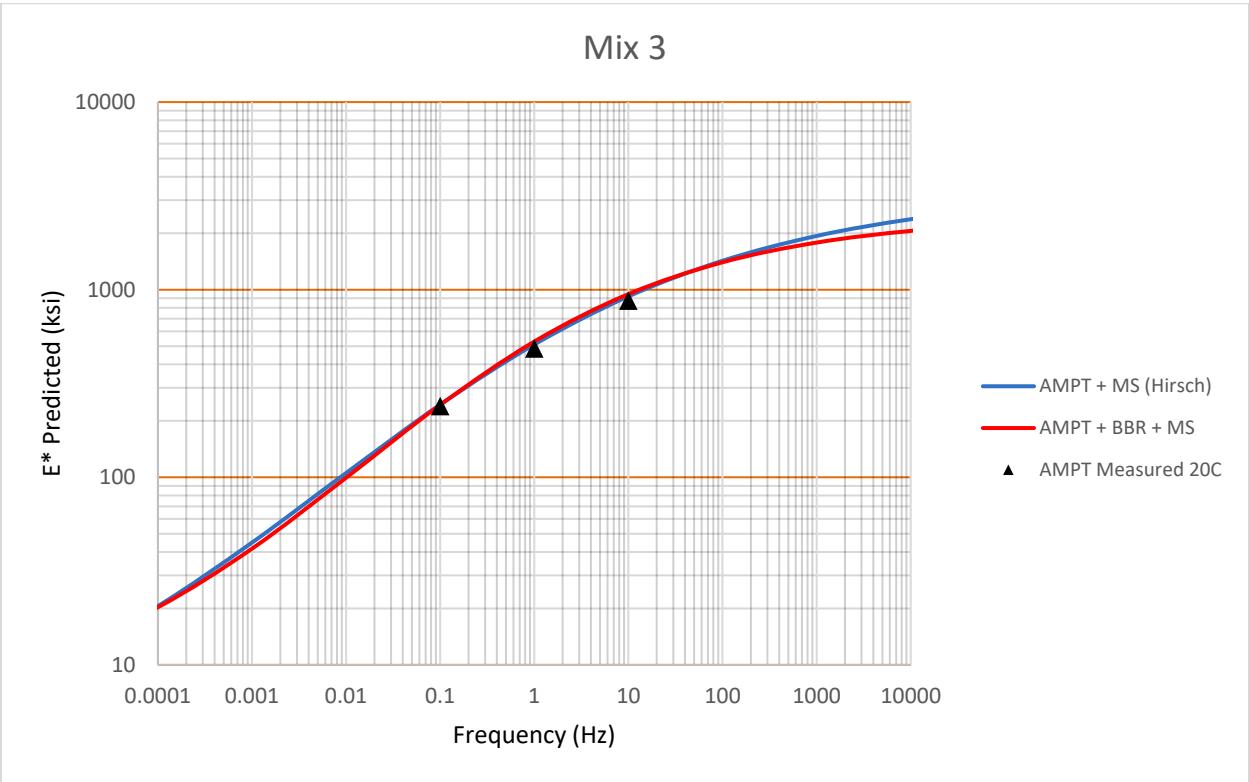
## References

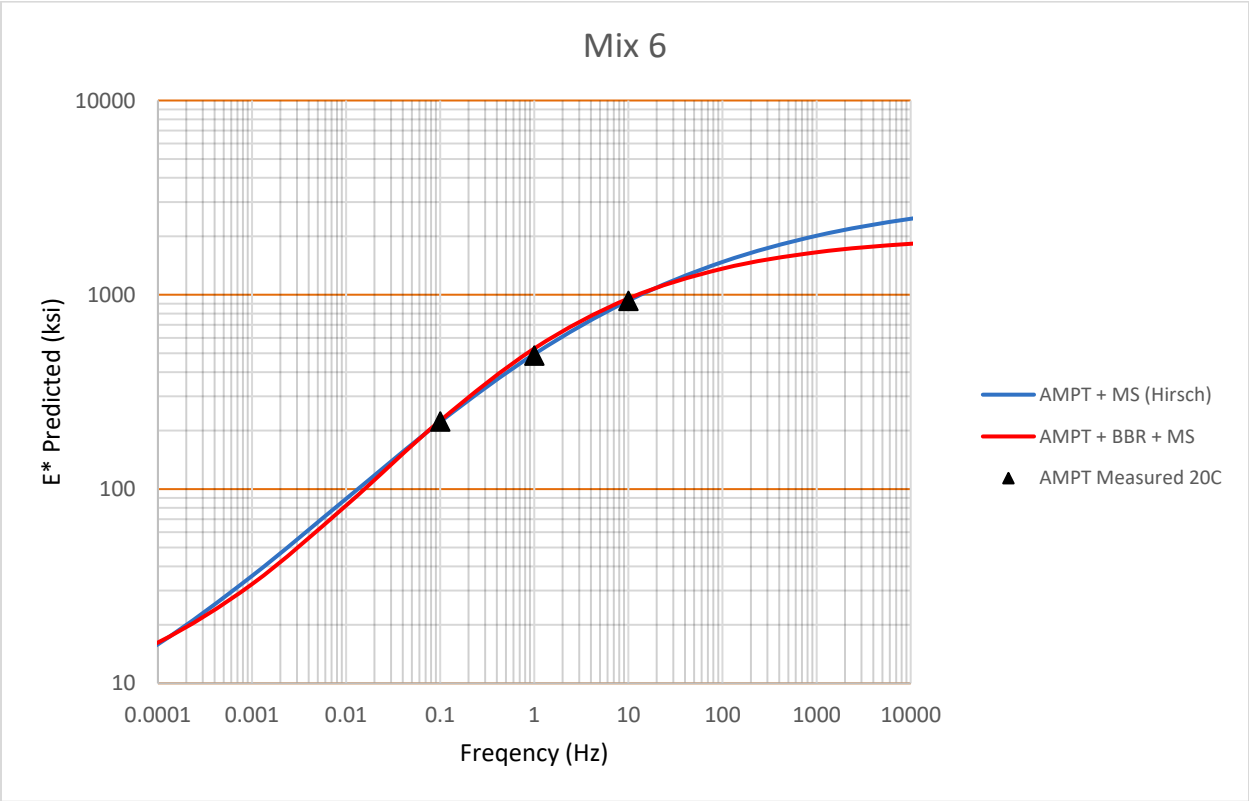
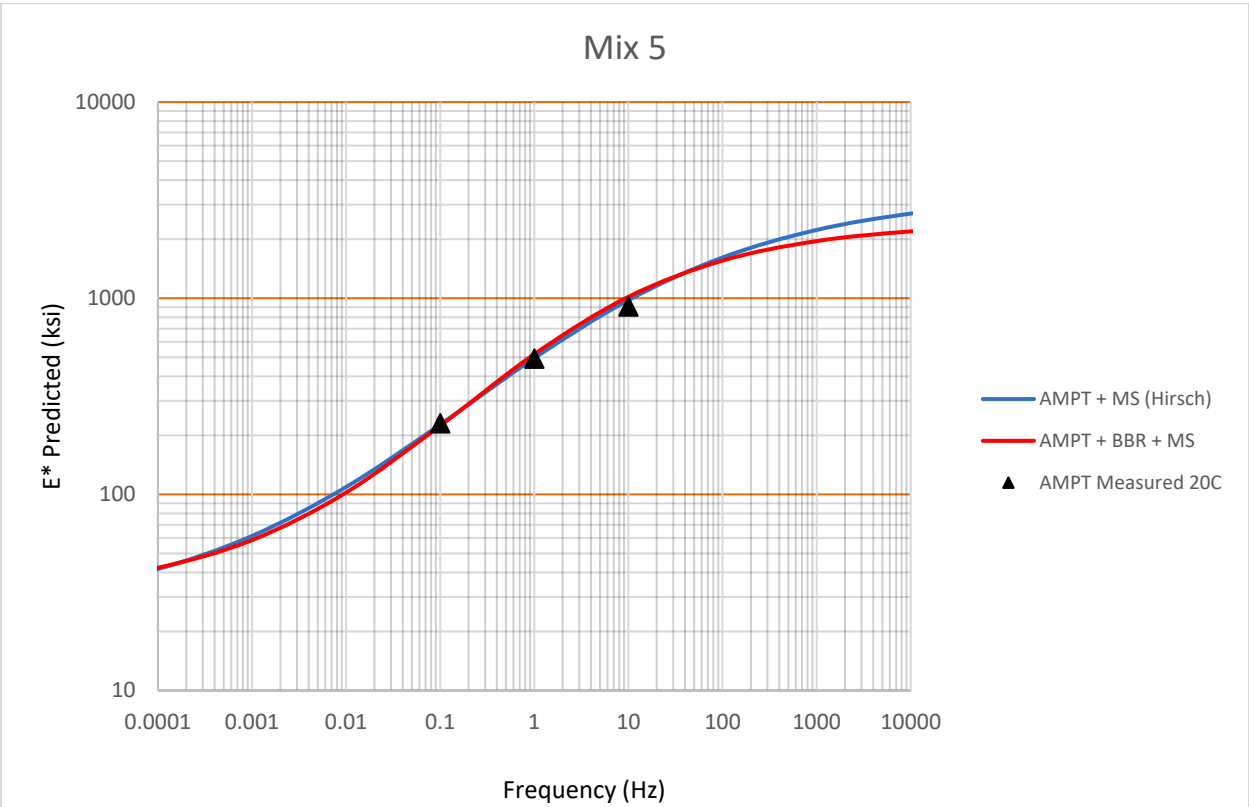
- [1] D. H. Timm, M. M. Robbins, N. Tran, and C. Rodezno, "Flexible Pavement Design – State of the Practice," Art. no. NCAT Report 14-04, Aug. 2014, Accessed: Apr. 12, 2025. [Online]. Available: <https://trid.trb.org/View/1322103>
- [2] W. Zhang, S. Shen, A. Faheem, P. Basak, S. Wu, and L. Mohammad, "Predictive quality of the pavement ME design program for field performance of warm mix asphalt pavements," *Construction and Building Materials*, vol. 131, pp. 400–410, Jan. 2017, doi: 10.1016/j.conbuildmat.2016.11.086.
- [3] P. Romero, K. VanFrank, University of Utah. Department of Civil and Environmental Engineering, and Mountain-Plains Consortium, "Modeling the Dynamic Modulus of Asphalt Mixtures Using Single-Value Test Results, Phase I: Initial Relation With Cracking Tolerance Index," UT-22.18, Oct. 2022. Accessed: Jun. 19, 2024. [Online]. Available: <https://rosap.ntl.bts.gov/view/dot/64691>
- [4] P. Romero-Zambrana *et al.*, "Modeling the Dynamic Modulus of Asphalt Mixtures Using Single-value Test Results Phase II: Relation Between E\* Parameters and CT Index," UT-24.02, Jan. 2024. Accessed: Jun. 19, 2024. [Online]. Available: <https://rosap.ntl.bts.gov/view/dot/73235>
- [5] M. R. Thompson, E. J. Barenberg, S. H. Carpenter, M. I. Darter, B. J. Dempsey, and A. M. Ioannides, "CALIBRATED MECHANISTIC STRUCTURAL ANALYSIS PROCEDURES FOR PAVEMENTS. VOLUME I - FINAL REPORT; VOLUME II - APPENDICES," Mar. 1990, Accessed: Jun. 25, 2025. [Online]. Available: <https://trid.trb.org/View/502452>
- [6] F. Zhou, S. Im, and S. Hu, "Development and Validation of the IDEAL Cracking Test," *Transportation Research Circular*, no. E-C251, Sep. 2019, Accessed: Jun. 29, 2024. [Online]. Available: <https://trid.trb.org/View/1666294>
- [7] M. R. Islam and R. A. Tarefder, *Pavement design: materials, analysis, and highways*. New York: McGraw-Hill, 2020.
- [8] W. Mogawer, T. Bennert, J. S. Daniel, R. Bonaquist, A. Austerman, and A. Booshehrian, "Performance characteristics of plant produced high RAP mixtures," *Road Materials and Pavement Design*, vol. 13, no. sup1, pp. 183–208, Jun. 2012, doi: 10.1080/14680629.2012.657070.
- [9] P. Romero and University of Utah. Department of Civil and Environmental Engineering, "Using the bending beam rheometer for low temperature testing of asphalt mixtures : final report.," UT-16.09, Jul. 2016. Accessed: Jun. 19, 2024. [Online]. Available: <https://rosap.ntl.bts.gov/view/dot/31113>
- [10] A. Zeinali, "Practice Makes Perfect: Preparing the AMPT Tests for Routine Use," *Asphalt*, vol. 29, no. 2, 2014, Accessed: Jun. 25, 2025. [Online]. Available: <https://trid.trb.org/View/1322283>

- [11] L. Roberts, P. Romero, K. VanFrank, and R. Ferrin, "Evaluation of Asphalt Mixture Performance Tester: Utah Experience," *Transportation Research Record*, vol. 2296, no. 1, pp. 69–76, Jan. 2012, doi: 10.3141/2296-07.
- [12] F. Zhou, Im ,Soohyok, Sun ,Lijun, and T. and Scullion, "Development of an IDEAL cracking test for asphalt mix design and QC/QA," *Road Materials and Pavement Design*, vol. 18, no. sup4, pp. 405–427, Nov. 2017, doi: 10.1080/14680629.2017.1389082.
- [13] Z. Jones, Romero, Pedro, and K. and VanFrank, "Development of low-temperature performance specifications for asphalt mixtures using the bending beam rheometer," *Road Materials and Pavement Design*, vol. 15, no. 3, pp. 574–587, Jul. 2014, doi: 10.1080/14680629.2014.908135.
- [14] R. Bonaquist and D. W. Christensen, "Practical Procedure for Developing Dynamic Modulus Master Curves for Pavement Structural Design," *Transp. Res. Rec.*, vol. 1929, no. 1, pp. 208–217, Jan. 2005, doi: 10.1177/0361198105192900125.
- [15] D. W. Christensen Jr, T. Pellinen, and R. F. Bonaquist, "HIRSCH MODEL FOR ESTIMATING THE MODULUS OF ASPHALT CONCRETE," in *Journal of the Association of Asphalt Paving Technologists*, 2003. Accessed: Jan. 17, 2025. [Online]. Available: <https://trid.trb.org/View/698821>

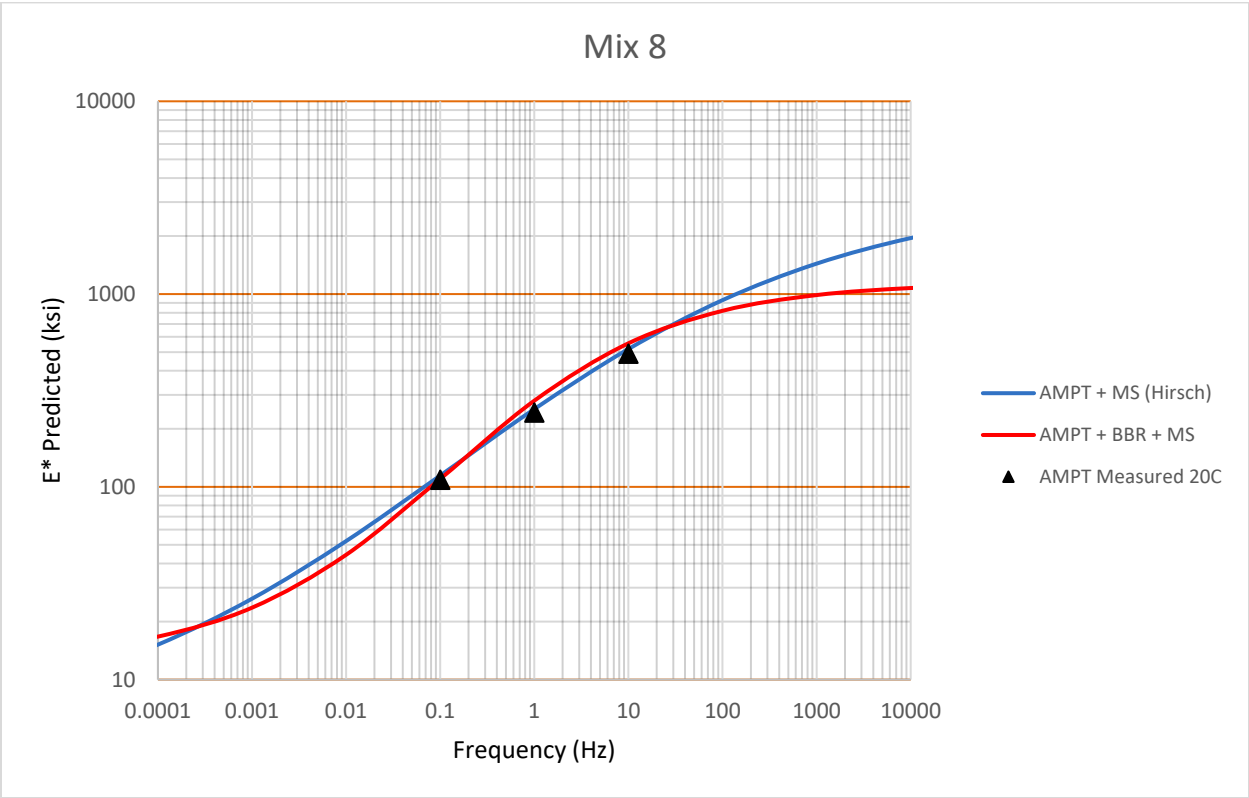
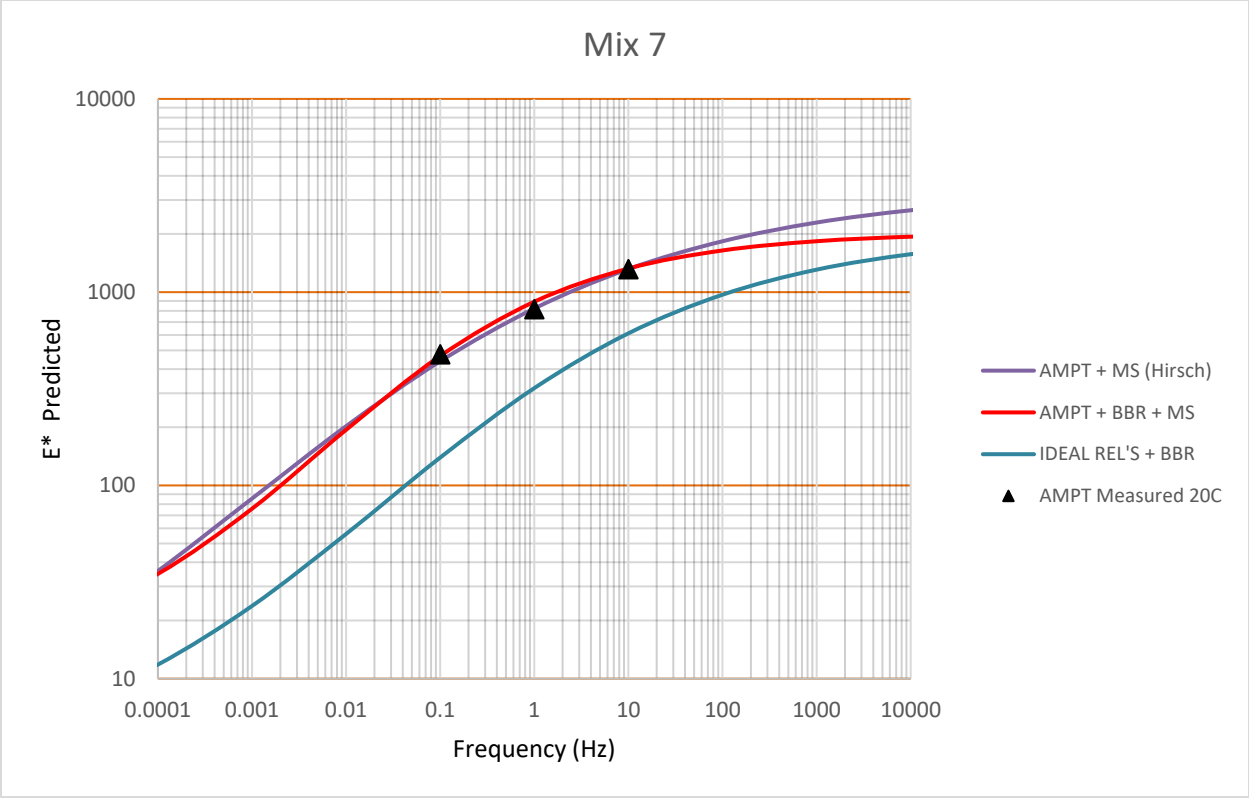
## Appendix A: Dynamic Modulus Master Curves

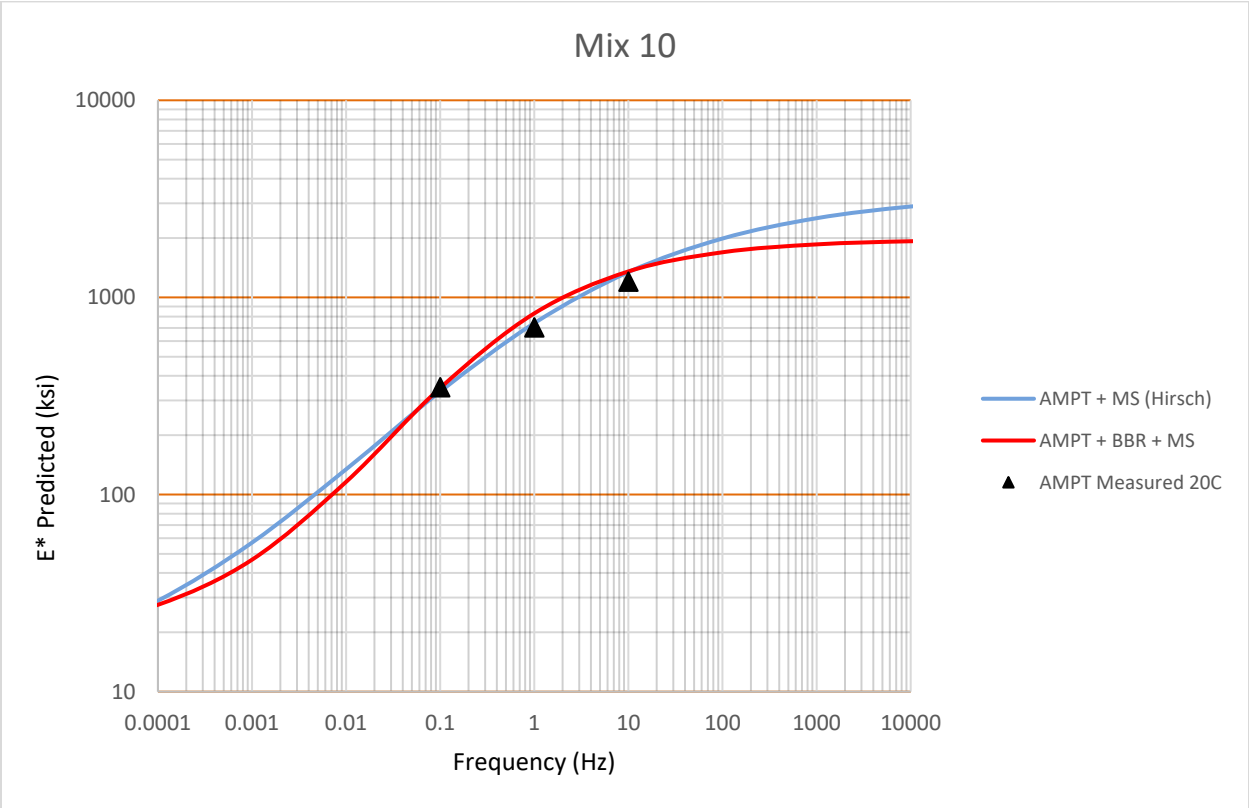
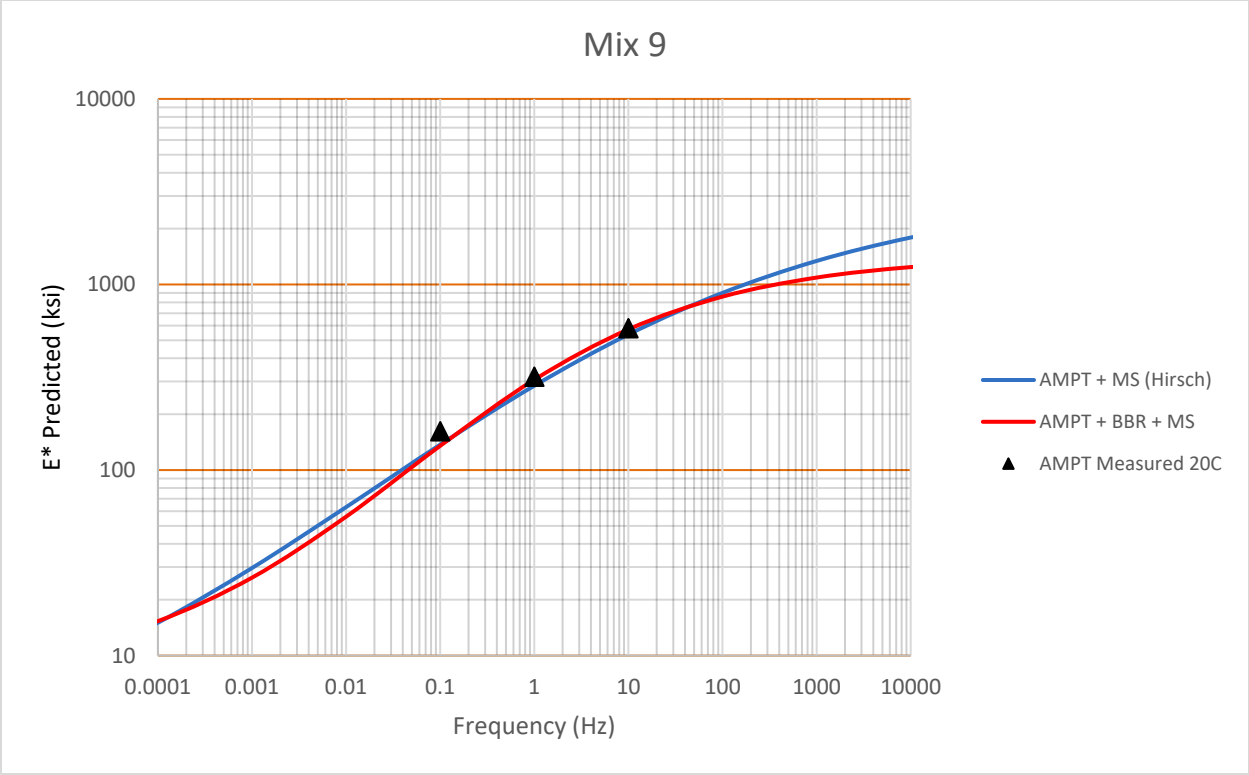


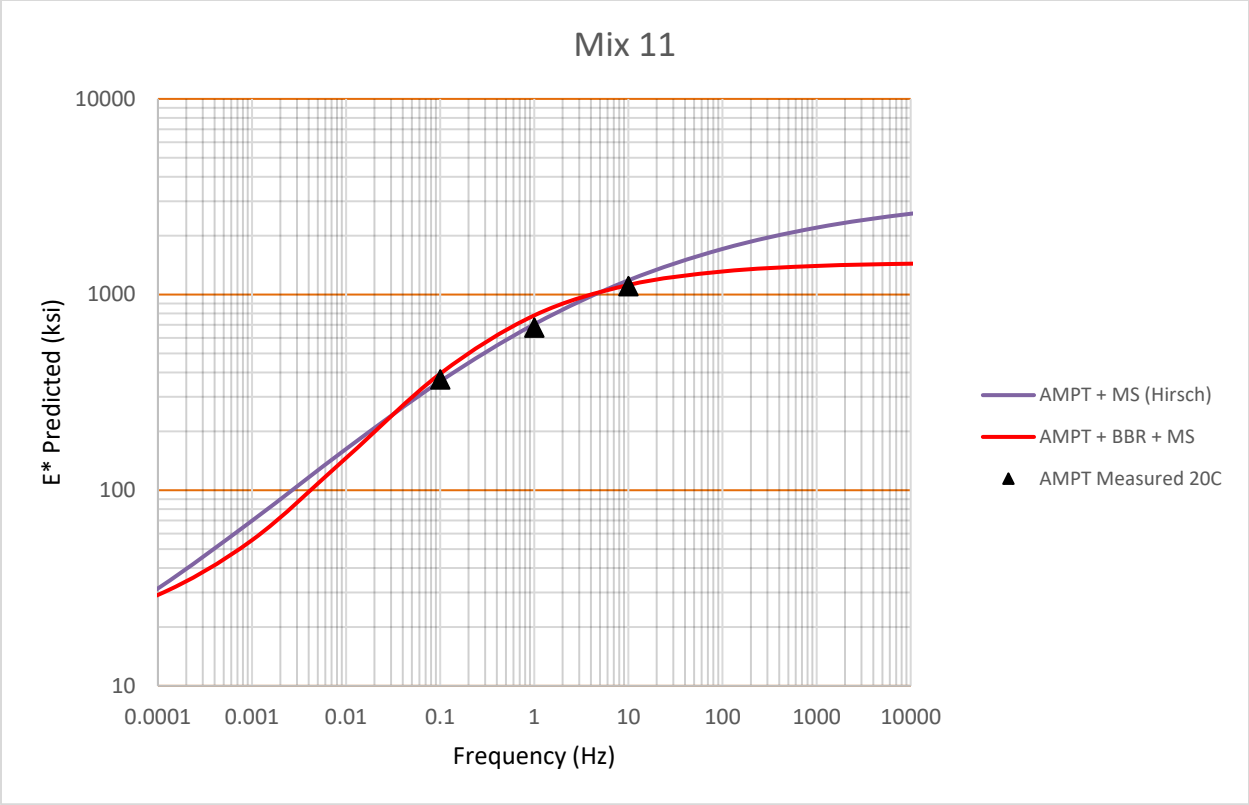












## Appendix B: Data Access

All of the data from testing was collected using electronic data acquisition of force, displacement, and temperature sensors. The data was collected in non-proprietary CSV format as generated by the data acquisition system. Spreadsheets were used to summarize and analyze the data. These data have been preserved and archived at Zenodo (<https://zenodo.org/>), an international repository/archive of research outputs from across all fields of research. Zenodo is listed as conforming to the USDOT Public Access Plan (<https://ntl.bts.gov/ntl/public-access/data-repositories-conformant-dot-public-access-plan>). According to Zenodo's policy, data entries remain accessible forever.

Dynamic Modulus Data was generated during Phase II of this study. The data can be accessed at the following link (presented here for completeness):

Romero, P. (2024). MODELING THE DYNAMIC MODULUS OF ASPHALT MIXTURES USING SINGLE-VALUE TEST RESULTS PHASE II: RELATION BETWEEN  $E^*$  PARAMETERS AND CT INDEX [Data set]. Zenodo. <https://doi.org/10.5281/zenodo.10501328>

A README file, including the metadata/information required to repeat the research, is included along with the data in the archive. Zenodo will provide proper citation for users to incorporate the data into their publications and will have a memorandum of understanding (MOU) stating that users may not re-release the data to a third party but direct them back to the repository.

New BBR data generated during the Phase III study is presented in Table 3 of this report.